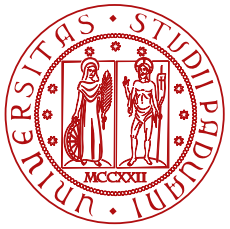

Università
degli Studi
di Padova

DIPARTIMENTO
DI INGEGNERIA
INDUSTRIALE

Master's Thesis in Aerospace engineering

Optical Performance Analysis of the SkyCompass-1 Telescope

Master's Candidate

Fraccaroli Pietro

Student ID 2061734

Supervisor

Prof. Giampiero Naletto

University of Padova

Academic Year
2023/2024

Contents

List of Figures

List of Tables

1 Introduction

The aim of this thesis is to provide clear guidelines on the manufacturing-alignment tolerances and performance of the Spock Ø250 space telescope on board the SkyCompass-1 satellite. These results will be shared with the engineering teams at Università degli studi di Padova, Officina Stellare, and Skyloom to facilitate the telescope's construction at Officina Stellare S.p.A. (Vicenza).

A technical and design-oriented approach was employed, focusing on feasibility considerations and optimizing the production and alignment costs of the telescope's various components.

The selection of optical tolerances was an iterative process, derived from numerous trials, constrained by mission requirements, and aimed at optimizing the telescope's performance.

The thesis is divided into two parts: the first four chapters describe the space mission, the telescope design, and the performance parameters. The second part analyzes three tolerance configurations using Monte Carlo simulations to determine the best option for implementation.

All studies were conducted using the Ray Tracing software Ansys - OpticStudio Zemax, licensed by University of Padova, and run on a standard laptop without the need for servers or additional computing power. The research began with a .zos (Zemax) file from Officina Stellare, which included the optical design of the telescope. All analyses of tolerances and performance assessments were carried out using this design, avoiding any major alterations, with only minor optimization suggestions offered.

1.1 Acronyms

AOI Angle of Incidence

FOV Field of View

FS Field Stop

GEO Geostationary Orbit

GTO Geostationary Transfer Orbit

IB Internal Baffle

IF Intermediate Focus

M1 Primary Mirror

M2 Secondary Mirror

MB Main Baffle

M1B Mirror 1 Baffle

M2B Mirror 2 Baffle

OD Optical Density

RC Ritchey-Chrétien

RMS Root-Mean-Square

SC1 SkyCompass-1

SF Solar Filter

WFE Wave Front Error

2 The mission: Skycompass-1

The American agency Skyloom Global Corp. (Colorado) is developing its first generation of laser communication geostationary small satellite constellations for GEO-LEO and GEO-GND data transfer. The first satellite, SkyCompass-1, is estimated to be launched in 2025. It will serve as the central node of a simple and responsive tactical lasercom data transfer network infrastructure, aiming to drastically increase the downlink capacity of sophisticated LEO-based Earth observation systems and enable real-time and high-resolution intelligence gathering.
Main features of the satellite mission:

- **Mission name:** SkyCompass-1 (SC1)
- **Geostationary Orbital slot:** 136°E
- **Telecommunication band (LEOP TT&C):** Ka Band
- **Satellite design, manufacture, assembly, and integration:** Performed in the US by Skyloom Global Corp. (Colorado)
- **Propulsion System:** Full chemical propulsion for orbit raising, momentum management, station keeping, and reorbit

3 Telescope Requirements

In Table (1), some of the mission requirements of the Spoke Ø250 telescope are listed. The telescope has numerous requirements; only those useful for our analysis have been reported here. After construction, the telescope must verify all requirements. Therefore, it is essential to study manufacturing and alignment tolerances in order to provide precise indications for telescope production to meet all required specifications. The most important performance requirement is 'REQ 9' and 'REQ 10': a very precise Wave Front Error is required after MAIT operations and in orbit. This requirement will be used to develop the entire tolerance study and utilized as a verification parameter to evaluate the performance of telescope configurations.

Table 1: Telescope Requirements

	Description	**Notes**
REQ 1	Wavelength 1550 nm	The system shall be optimized at a wavelength of 1550 nm +/-5 nm
REQ 2	Wavelength Range C-Band	The system shall be able to transmit and receive wavelengths along the C-band: 1525 nm to 1575 nm without significant degradation in throughput and performance.
REQ 3	Telescope Aperture	The aperture of the system shall be 250 mm +1.00 / -0.00 mm in diameter
REQ 4	L3 – Exit Pupil Distance	The distance between the last vertex of lens L3 and the Exit Pupil position shall be greater than 68 mm and not greater than 80 mm
REQ 5	Field of View	The unvignetted Field of View half-angle (FOV) on-sky of the system shall be 0.2 deg +0.05 /-0.00 deg measured from the telescope optical axis.
REQ 6	Absolute Trasmission	The Absolute transmission at system wavelengths indicated in [REQ. 2], shall be greater than 90%
REQ 7	Avarage Trasmission	The Average transmission at system wavelengths indicated in [REQ. 2], shall be greater than 95%
REQ 8	Field Stop	The intermediate focus of the system (diffraction limited focus) shall be nearly at vertex of the primary mirror as possible. The Field Stop (FS) shall be located in such position and must limit the FOV to 0,3 deg
REQ 9	WFE after MAIT	The Wave Front Error Root-Mean-Square (WFE RMS) shall be not greater than 80 nm measured at 20 ºC after MAIT procedures for wavelengths indicated in [REQ. 2] within the entire FOV indicated in [REQ. 5]
REQ 10	WFE in Orbit	The WFE RMS shall not be greater than 100 nm considering Gravity Release effects when the telescope has uniform temperatures within the operative temperatures for wavelengths indicated in [REQ. 2] within the entire FOV indicated in [REQ. 5]

3.1 Wave Front Error

The Root Mean Square (RMS) Wavefront Error is a quantitative measurement of wavefront aberrations in an optical system. This parameter is crucial for evaluating and optimizing the performance of a telescope, ensuring high-quality and precise images.
Fundamentally, the RMS Wavefront Error provides a numerical representation of how closely the actual wavefront of an optical system aligns with a perfect spherical wavefront. The calculation involves comparing the real wavefront deviations with an ideal reference, using a formula that captures the statistical average of the squared deviations. This result succinctly quantifies the optical imperfections across the entire wavefront.

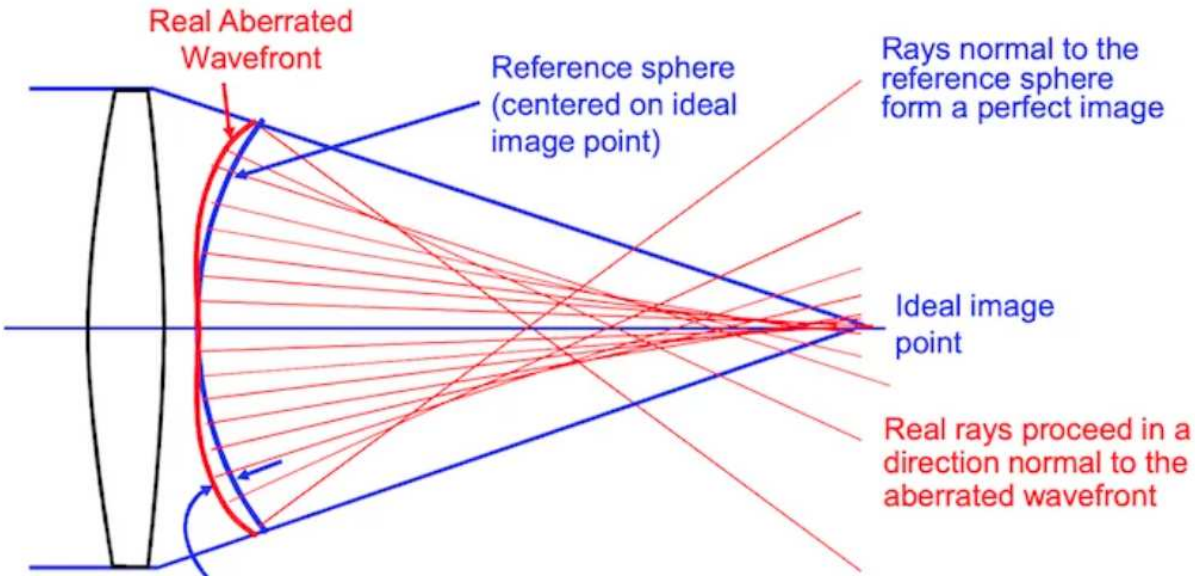

Figure 1: WaveFront Error (WFE): difference from real wavefront (red) and a spherical reference wavefront (blue) - credits: opticsforhire.com

The RMS Wavefront Error represents the root mean square deviation of the actual wavefront from an ideal wavefront. The calculation formula considers the statistical average of the squared deviations from the ideal reference.

$$\text{RMS WFE} = \sqrt{\frac{1}{N}\sum_{i=1}^{N}\left(WFE_i - \overline{WFE}\right)^2}$$

where:

N = Total number of points measured on the wavefront

WFE_i = Wavefront error value at a specific point

$\overline{WFE}$ = Mean value of the wavefront, calculated as: $WFE = \frac{1}{N}\sum_{i=1}^{N} WFE_i$

The error is expressed as the square root of the difference between the average of the squared deviations and the square of the mean deviation, clearly quantifying the optical imperfections along the entire wavefront. The RMS value expresses the statistical deviation from a perfect reference sphere, averaged over the entire wavefront. Wavefront aberration refers to deviations from an ideal optical wavefront, manifesting as distortions or imperfections in the propagation of light waves through an optical system. These aberrations can impact image quality and the overall performance of optical instruments, making their understanding and measurement crucial in the field of optics.

3.1.1 Wavefront Map

A valuable tool available in OpticStudio for wavefront analysis is the Wavefront Map, which illustrates the difference in the wavefront at the exit pupil compared to the ideal shape. The wavefront map is a visual representation of the aberrations present in an optical system. This map displays the deviations of the real wavefront from an ideal wavefront across the entire optical system. In essence, the wavefront map is a graphical representation showing how light propagates through the optical system, highlighting the distortions or irregularities that can impact image quality. Each point on the map corresponds to a specific position of the wavefront at the exit pupil and indicates the magnitude and direction of the deviation from the ideal shape.

In the graphs in Figure(2), wavefront map of the telescope is represented. The darkening due to the M2 Mount (spider arms) composed of three arms is immediately noticeable (for mechanical design see figure (5)). From the analysis of the map, we can obtain the WFE Peak

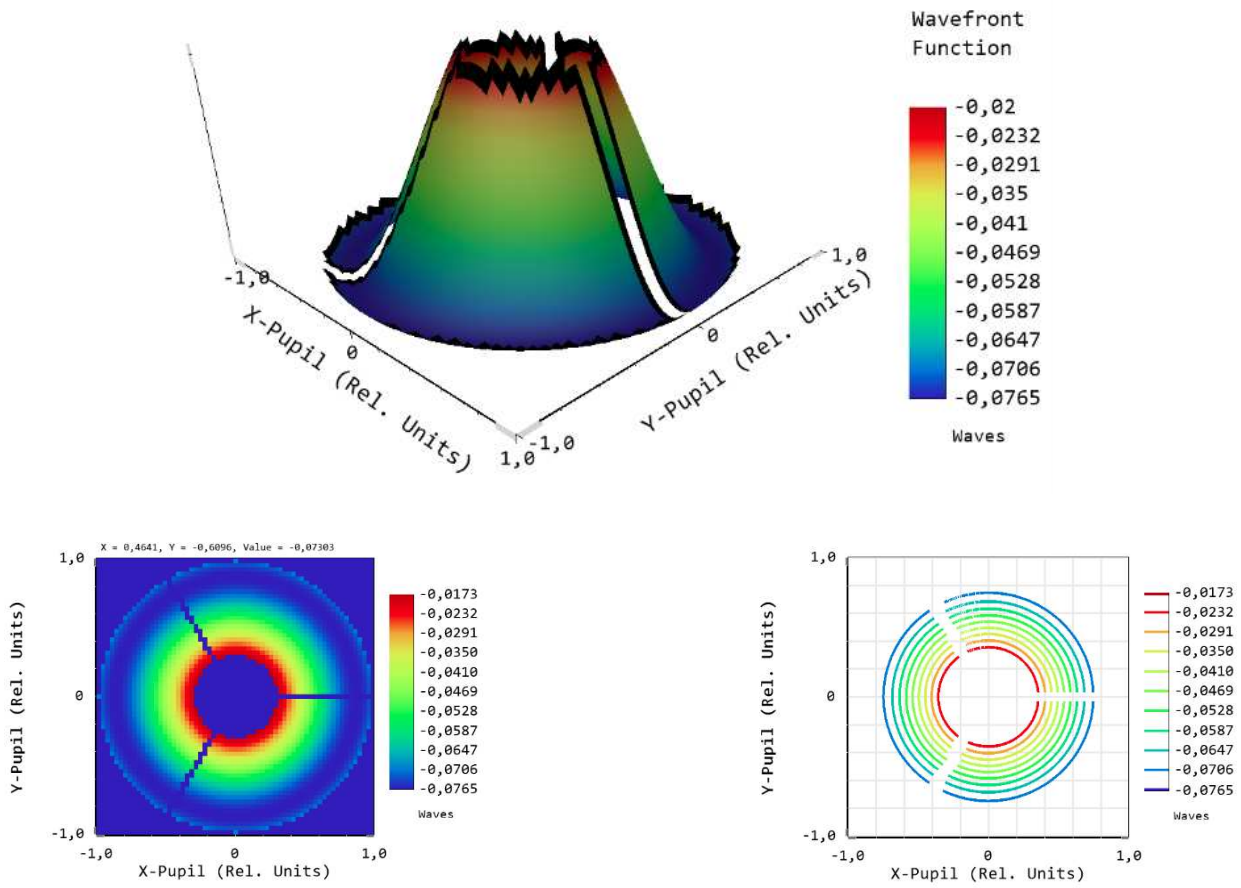

Figure 2: Spock Ø250 WaveFront Map: different visualization from OpticStudio "Wavefront Map" tool. All value are expressed in waves ($\lambda = 1550$nm).

to Valley (PV) value, which indicates the difference between the maximum and minimum WFE extremes. Additionally, the software calculates the RMS WFE, yielding the following results:

- The WFE Peak to Valley value is: $WFE\_PV = 0.059\lambda = 91.45$ nm
- The RMS WFE value is: $WFE\_RMS = 0.022\lambda = 34.10$ nm
- The Exit Pupil diameter is: $EP\_diam = 7.50$ mm

3.2 Diffraction considerations

Diffraction is a fundamental factor in the analysis of high-precision optical systems. According to wave optics theory, every optical system experiences diffraction effects that limit its resolving power. Diffraction results in a point source being imaged not as an infinitesimally small point but as a finite-sized Airy disk. The Airy disk is the diffraction pattern produced by a point source when focused by an ideal optical system. An optical system is termed diffraction-limited when its resolution is constrained by diffraction effects, rather than by imperfections or aberrations in the lenses or other optical components. This means the system's performance is at the theoretical limit imposed by the wave nature of light, achieving the highest possible resolution for a given aperture size. To evaluate whether an optical system is diffraction-limited, we can use the Strehl ratio. The Strehl ratio is a measure of the quality of optical image formation. It is defined as the ratio of the peak intensity of an aberrated image (produced by a real optical system) to the peak intensity of an ideal, diffraction-limited image (produced by a perfect optical system without any aberrations). Mathematically, the Strehl ratio S can be expressed as:

$$S = \frac{I_{\text{aberrated}}}{I_{\text{ideal}}}$$

where:

- $I_{\text{aberrated}}$ is the peak intensity of the image formed by the actual optical system with aberrations.
- I_{ideal} is the peak intensity of the image formed by an ideal diffraction-limited optical system.

The Strehl ratio (S) can be also defined as follows:

$$S = \frac{\left|\int_A P(x,y) e^{i\phi(x,y)}\, dA\right|^2}{\left|\int_A P(x,y)\, dA\right|^2}$$

where:

- A is the aperture of the optical system,
- $P(x,y)$ is the pupil function, describing the amplitude of the wavefront across the aperture,
- $\phi(x,y)$ is the wavefront phase error across the aperture.

The Strehl ratio (S) can be expressed in terms of RMS WFE as follows:

$$S = \exp\left(-\left(\frac{2\pi\Delta\phi}{\lambda}\right)^2\right)$$

where:

- $\Delta\phi$ is the RMS (Root Mean Square) phase error of the optical wavefront,
- λ is the wavelength of the light.

This approximate model describes the Strehl ratio in terms of the RMS phase error, which represents the aberrations present in the optical system. The Strehl ratio ranges from 0 (aberrated) to 1 (diffraction-limited). As the RMS wavefront error increases (indicating more significant aberrations), the Strehl ratio decreases exponentially according to the equation. This implies that even small amounts of wavefront error can significantly impact image quality.
According to Maréchal's criterion, an optical system is considered diffraction-limited if its Strehl ratio is greater than 0,8.

$$\exp\left(-\left(\frac{2\pi\Delta\phi}{\lambda}\right)^2\right) > 0,8$$

Thus, by solving the equation associated, we obtain that

$$\Delta\phi = 0,075\lambda$$

In our case $\lambda = 1550$ nm, so in terms of nanometers

$$\Delta\phi = 116 \text{ nm}$$

We obtain diffraction limit value in term of RMS WFE: $0,075\lambda = 116$ nm.
Therefore, we can conclude that the instrument is diffraction-limited.
As already discussed, the geometrical aberrations of the telescope, as obtained from ray tracing, are well below the diffraction limit of 0.075 lambda. The requirement limit of 80nm (0.052 λ) is also below the diffraction limit.
In terms of RMS WFE we can compute geometric aberration and diffraction contribution.

Therefore, the nominal WFE inclusive of diffraction is:

$$RMS\_WFE\_nominal = 0,022\lambda = 34\text{nm}$$

$$\sqrt{0.022^2 + 0.075^2} = 0.078\lambda = 121 \text{ nm}$$

$$S = 0.79 \text{ Strehl ratio}$$

The acceptable limit indicated by requirement of 80 nm instead is:

$$RMS\_WFE\_req = 80\text{nm} = 0,052\lambda$$

$$\sqrt{0.052^2 + 0.075^2} = 0.091\lambda = 141 \text{ nm}$$

$$S = 0.72 \text{ Strehl ratio}$$

In practice, the requirement accepts a performance degradation equivalent to 9-10% of the Strehl ratio.

4 Spock Ø250mm Telescope: Optical and Mechanical Design

4.1 Optical Design

Figure 3 shows the optical surfaces where ray-tracing simulations will be conducted. Mirrors M1 and M2, along with lenses L1, L2, L3, are represented in black. Incident rays are coloured in blue, all parallel to the telescope's axis with an angle of incidence of 0° (0° FOV).

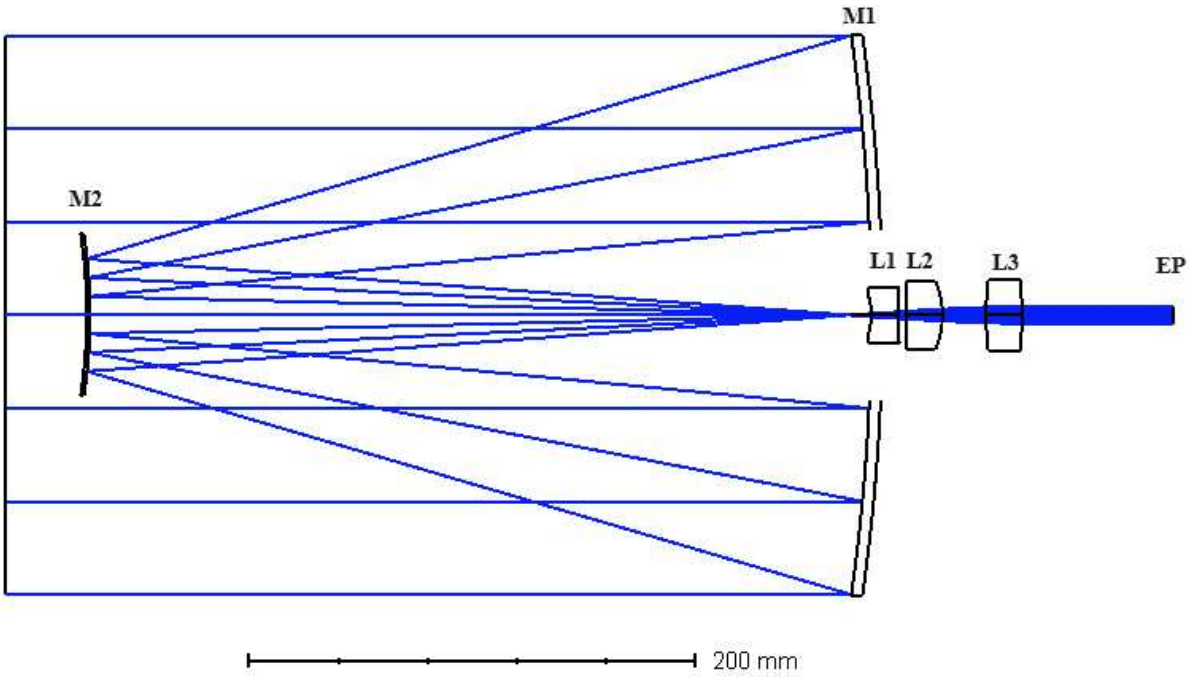

Figure 3: Optical design layout of Spock Ø250 Telescope - OpticStudio

Below, the main characteristics of the mirrors, lenses, solar filter, and field stop are presented.

4.1.1 Mirrors

The telescope features a Ritchey-Chrétien configuration in which both mirrors are hyperbolic: the primary mirror is concave and the secondary mirror is convex. Both mirrors are made of aluminum and are coated with unprotected gold. The telescope is on-axis, meaning all optical elements are nominally perpendicular to the telescope's axis. The relative distance between

the two mirrors is 350 mm. Additional characteristics, such as the radius of curvature of the surface, conic constant, and semi-diameter, which define the size, can be seen in Table 2.

Mirror	Radius [mm]	Distance [mm]	Coating	Semi-Diameter [mm]	Conic	Material
M1	-875.00	-350.00	Gold	125.24	-1.03	Aluminum
M2	-235.637	350.00	Gold	36.32	-3.28	Aluminum

Table 2: Characteristics of the primary (M1) and secondary (M2) mirrors.

4.1.2 Lenses - Eyepiece Assembly

Continuing along the optical path, following the primary mirror (M1) and the secondary mirror (M2), we encounter the Eyepiece Assembly consisting of spherical lenses L1, L2, and L3, which collimate the light beam to create an afocal system. This results in a collimated beam where the Exit Pupil is positioned at a nominal distance of 70 cm (See 'REQ 4'). The calculated diameter of the Exit Pupil is Ø7.5 mm. This location is where the Infrared Sensor/Transmitter will be mounted.

Lens	Radius A [mm]	Radius B [mm]	Thickness [mm]	Semi-Diameter [mm]	Material
L1	-28.98	164.38	12.05	12.51	SK - 1300
L2	-334.51	-38.40	16.12	15.30	S – LAL20
L3	132.65	-141.61	16.03	15.95	S – LAH58

Table 3: Characteristics of lenses L1, L2, and L3.

As shown in the table 3, various data about the lenses can be found, including their materials:

- L1: "SK-1300" is a glass composed of fused silica glass;
- L2: "S-LAL20" is a glass based on Lanthanum and Aluminum;
- L3: "S-LAH58" is a glass based on Lanthanum.

The columns "Radius side A" and "Radius side B" indicate the curvature radii of both sides of each lens. Progressing along the optical path, after encountering mirrors M1 and M2, the light beam passes through side A of L1 and exits from side B. The approximate dimensions of the Eyepiece Assembly are those of a cylinder with a diameter of 3.2 cm and a height of 7 cm. Here, a mechanism for calibrating the relative position between the Assembly and the mirrors must be provided during the alignment campaign to achieve the desired performance and mitigate the negative effects due to tolerances.

4.1.3 Solar Filter

To manage the telescope's thermal conditions when exposed to sunlight and to shield its internal optical components from the radiative environment of space and potential contamination from the ground, a Solar Filter (SF) is placed at the telescope's entrance. This filter is made up of a flat glass window with appropriate coatings. A dedicated section on the study of the Solar Filter will be discussed in this thesis.

4.1.4 Field Stop

As shown in Figure.4, the Ritchey-Chrétien configuration generates an intermediate focus (IF) near M1. A Field Stop is planned to be positioned at the intermediate focus to limit the Field of View (FOV) to 0.3 degrees [REQ 8] (1). The purpose of the field stop is to reduce field aberrations, increase image sharpness and contrast, and decrease stray light.

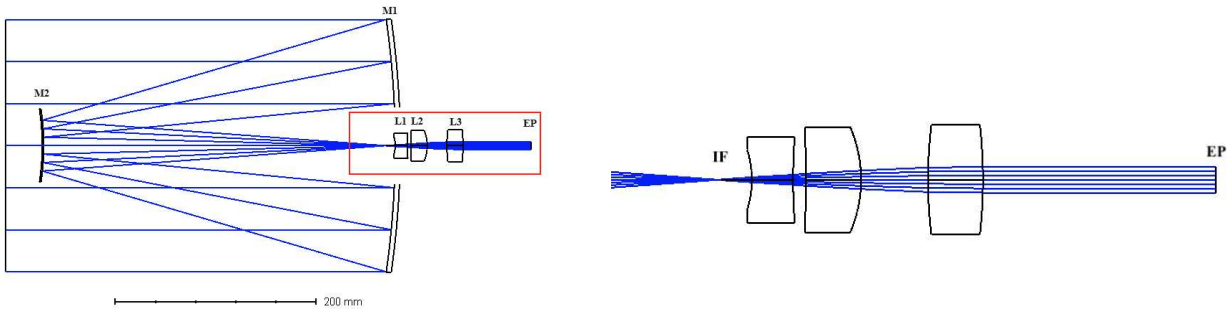

Figure 4: Field stop position: intermediate focus

4.1.5 Afocal System

An afocal telescope offers several specific advantages for space optical telecommunications, as in our case, both for the reception and transmission of laser beams. Here are some of the

main benefits:

1. **Beam collimation over long distances:** An afocal telescope is designed to transform a parallel light beam into another parallel light beam, maintaining laser beam collimation over long distances. This is crucial for space communications, where signals must travel across vast stretches of space without dispersing.

2. **Increased angular resolution:** Using an afocal system improves angular resolution, allowing precise discrimination and targeting of laser signals. This is essential for the accurate transmission and reception of data between satellites or between a satellite and a ground station.

3. **Minimization of optical aberrations:** Afocal telescopes can be designed to reduce optical aberrations, such as astigmatism and distortion. This enhances the quality of the received or transmitted laser signal, ensuring that data transmission remains clear and consistent.

An afocal telescope offers numerous advantages for space optical telecommunications, enhancing beam collimation, angular resolution, and signal quality. Their ability to reduce optical aberrations and beam divergence makes them ideal tools for ensuring efficient and reliable transmission and reception of laser signals in space.

4.2 Mechanical Design

In figure (5), we can clearly see, along with mirrors and lenses, the mechanical components of the telescope: mounts, baffles, and the Backplate to which all parts of the telescope are connected.

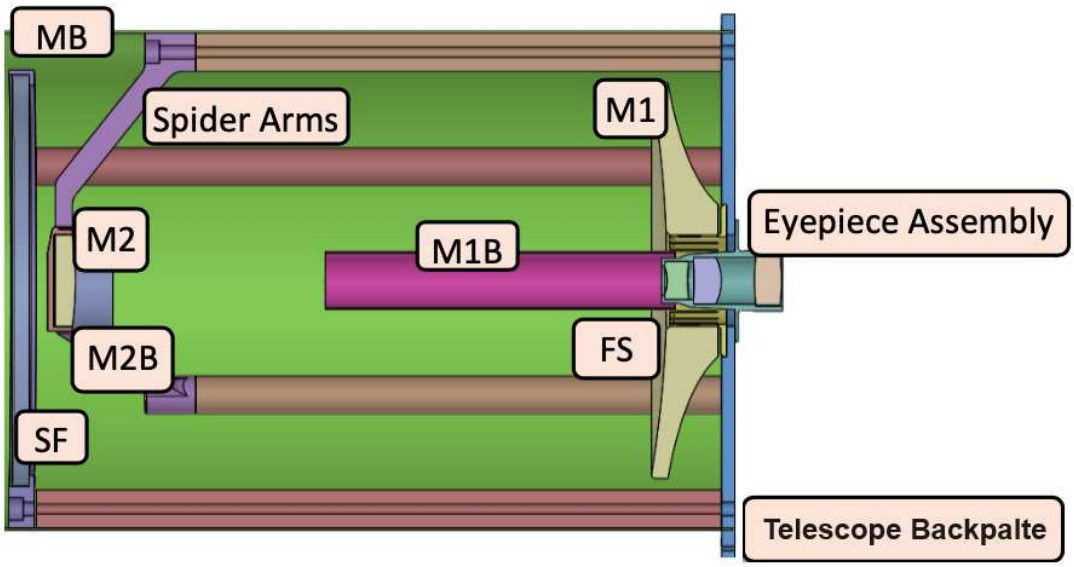

Figure 5: Mechanical design layout of Spock Ø250 Telescope - credits: Skyloom

4.2.1 General features

The telescope dimensions and mechanical configuration are detailed in figure 6: it can be observed that the telescope length, measured from the solar filter SF to the Telescope mounting plane (Backplate), does not exceed 475 mm. Additionally, 130 mm are considered from the Backplate to the exit pupil. The diameter of the Main Baffle of the telescope must be less than 330 mm, and the Backplate diameter must be within 440 mm.
The telescope's mass must not exceed 17 kg.
Materials used for different telescope components, including adhesives, paints, and surface treatments, must be suitable for the space environment, ensuring minimal deterioration of their optical and mechanical properties. It is important to note that the mission involves 5 years in GEO.

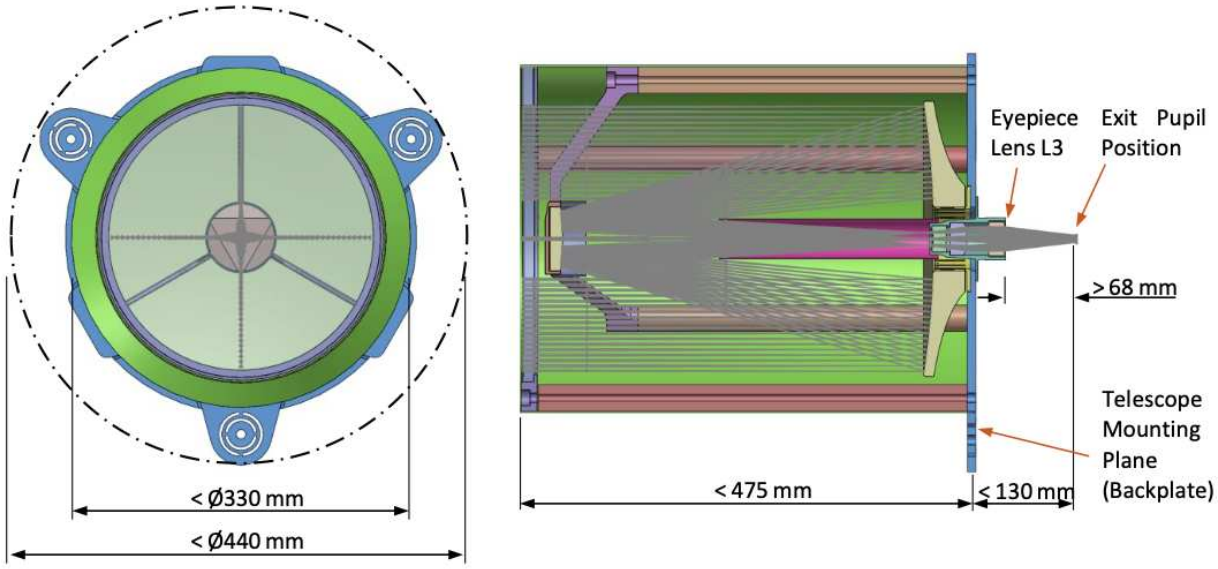

Figure 6: Lengths of interest for the definition of the telescope envelope - credits: Skyloom

4.2.2 Baffles

As shown in Figure 5, the instrument features a Main Baffle (MB) that protects the entire telescope, and two internal baffles:

- M1B: An internal baffle located between the primary and secondary mirrors.
- M2B: An internal baffle surrounding the M2 mirror.

The primary purpose of these baffles is to mitigate stray light. MB, M1B and M2B surface present grooves. These are designed to eliminate grazing-angle reflections and shall have a pitch of 1 mm and be 0.5 mm in depth, as presented on (!!da aggiungere FIGURE!!). Appropriate coatings, such as MAP-AQ-PU1 for non-flat surface or Acktar Metal-Velvet for flat surface, are used to create black surfaces, meeting the following requirements: minimizing electrical conductivity, maximizing absorption, minimizing emissivity, and having low outgassing values. The following surfaces are treated with black paint:

- Spider: Inner surfaces.
- MB: Internal surface.
- M1B: Internal and external surfaces.
- M2B: Internal surface (not in contact with M2 substrate), external surface.

- M2 Bolts Cap: External surface.
- FS: Both sides.

4.2.3 Mounts

The primary Mirror M1 is positioned on a mount directly connected to the telescope structure on the Backplate, while mirror M2 is positioned via a three-arm spider mount and is directly connected to the Backplate.
Lenses L1, L2, L3, divided by spacers, are located within the eyepiece assembly, which is fixed directly to the Backplate too.

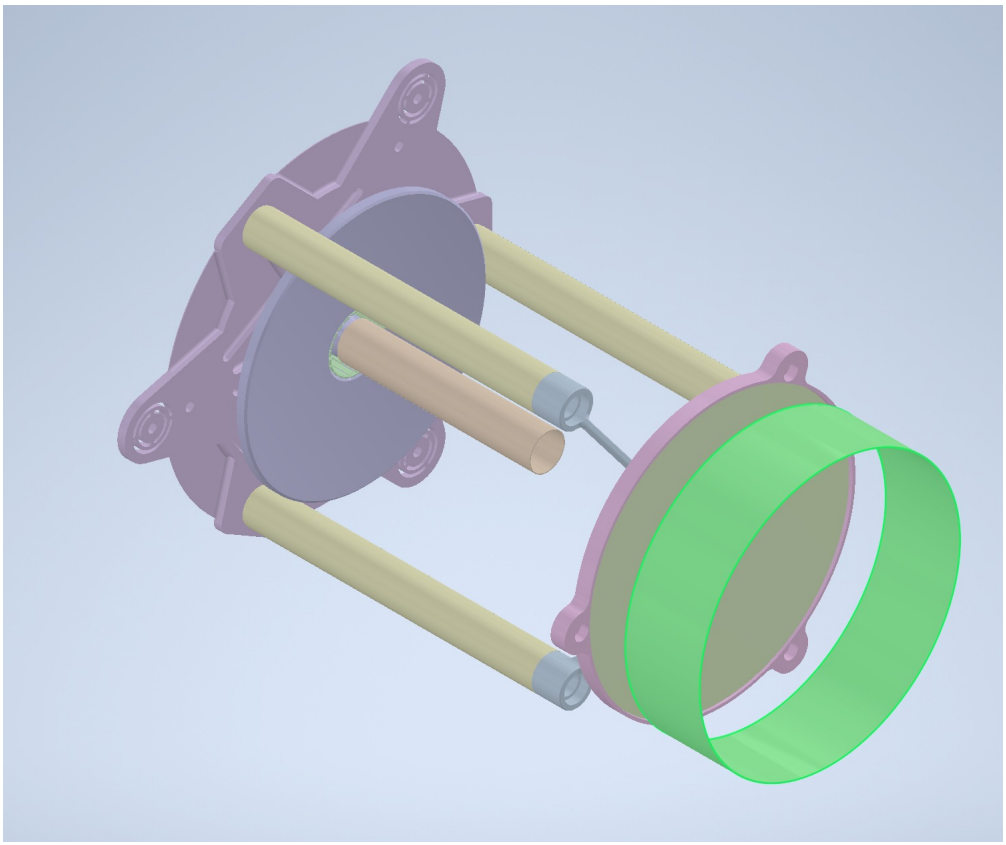

Figure 7: CAD layout of Spock Ø250 Telescope - credits: Skyloom

4.3 Telescope performance

The performance analysis of the telescope in terms of RMS WFE has already been discussed. This paragraph focuses on the spot diagram. To conduct this analysis, the tools provided by the OpticStudio software are utilized. However, it is important to keep in mind that we are working with an afocal instrument operating at monochromatic wavelength. This context must be considered to ensure accurate interpretation of the results and to account for the specific characteristics and limitations inherent to the telescope's design.

4.3.1 Paraxial Focus

To quickly and effectively characterize the performance of the telescope, a paraxial optic is used to focus the collimated beam from the Eyepiece Assembly onto a focus located 100 mm away from the Eyepiece. This paraxial optic is an ideal surface that does not introduce aberrations, providing a pure evaluation of the telescope's optical performance without the additional complications of optical defects. The paraxial optic is temporarily introduced exclusively for evaluating the instrument's performance, providing a clear and accurate representation of the optical system's behavior. By using this technique, it is possible to precisely focus the light beam and subsequently evaluate the Spot Diagram. The Spot Diagram provides a visual representation of the distribution of focused light points, revealing potential aberrations and the quality of the image produced by the telescope.

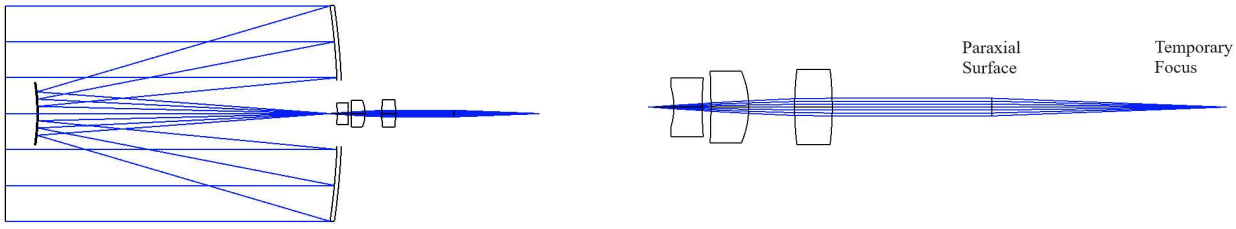

Figure 8: Paraxial Surface - OpticStudio

4.3.2 Spot Diagram analysis

The spot diagram is a fundamental tool in analyzing the optical performance of a telescope. It provides a visual representation of the distribution of light points on the focal plane, resulting from the passage of light rays through the telescope's optical system. Each point on the spot

diagram represents where a light ray from an object point is focused after passing through the telescope's optical surfaces. This tool allows for the evaluation of various aspects of image quality, including the effects of optical aberrations such as spherical aberration, coma, and astigmatism. By analyzing the spot diagram, it is possible to determine the accuracy of the telescope's focus and identify any optical issues that may affect the quality of observed images.

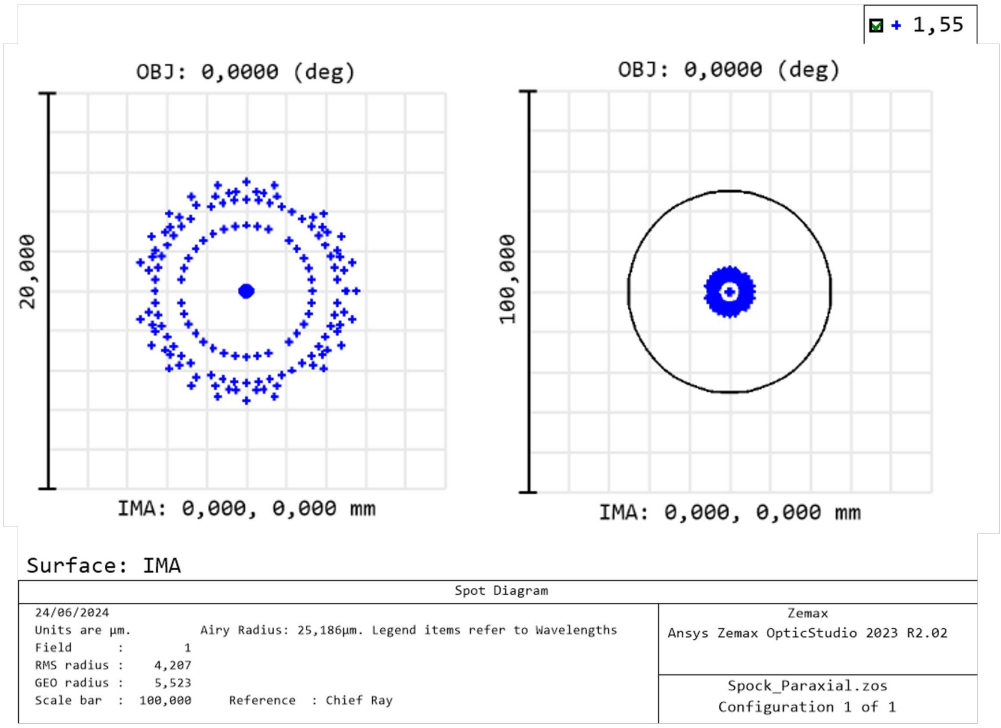

Figure 9: Standard Spot Diagram -OpticStudio

In the image (9), we can observe the representation of two spot diagrams generated by OpticStudio. A single Field of 0° (on axis) is analyzed. The spot diagram on the left is similar to the one on the right, except that the latter has highlighted the Airy disk (black circle) and has therefore been rescaled. The blue dots represent the individual ray traces that have been simulated through the optical system. These rays are typically traced from different points on the entrance pupil.
From the spot diagram, we can derive some information:

- **RMS radius** = 4,207 μm
  The RMS spot radius is the root-mean-square radial size. The distance between each ray and the centroid is squared, and averaged over all the rays, and then the square

root is taken. The RMS spot radius gives a rough idea of the spread of the rays, since it depends upon every ray.

- **GEO radius** = 5,523 μm
  The GEO spot radius is the distance from the reference point (centroid) to the ray which is farthest away from the reference point. In other words, the GEO spot radius is the radius of the circle centered at the reference point which encloses all the rays.

- **Airy disk**: all the rays are within the Airy disk. As we already discussed, the system is diffraction limited.

- **Dimensions and symmetry**: small size of the spot diagram indicate a very low presence of spherical aberration, suggesting that this is a high-precision monochromatic optical system. Since we are in an on-axis configuration, we expect a symmetrical spot diagram, as confirmed by the figure.

5 Tolerance Analysis

Tolerance analysis in a high-precision optical system is a crucial phase to ensure the feasibility, performance, and capability of the manufacturing and alignment of the telescope components. This analysis allows for identifying and quantifying manufacturing and assembly errors that can negatively impact the overall performance of the instrument.
In a complex optical system, each component can have manufacturing defects or alignment errors, which could significantly compromise the quality of the produced image. For this reason, it is essential to conduct a detailed tolerance analysis campaign during the design phase. This process helps determine the actual capability to produce the instrument with the desired performance and estimate the associated production and alignment costs.
The tolerances considered in this study are primarily of two types:

- **Manufacturing Tolerances:** These tolerances are the deviations in the production processes of optical components. They include variations in dimensions, shape, radius of curvature, and surface finish of lenses and mirrors. Manufacturing tolerances are crucial to ensure that each component meets the design requirements.

- **Alignment Tolerances:** These tolerances refer to the allowable deviations during the assembly and alignment of optical components. Alignment tolerances are important to maintain the correct position and orientation of components within the system, ensuring that light rays follow the nominal optical path without significant deviations.

To combine the simultaneous effect of tolerances for all elements, two main calculation tools are used:

- **Sensitivity Analysis:** This technique evaluates the impact of variations in each tolerance on the performance parameters of the optical system. By identifying the components or tolerances that most affect image quality, sensitivity analysis allows manufacturers to prioritize production and alignment efforts for the greatest impact. These tolerances are called "Worst Offenders". A detailed analysis of these parameters is essential for identifying the main sources of error and determining where increased precision is necessary.

- **Monte Carlo Analysis:** This statistical technique simulates a large number of random tolerance scenarios to evaluate the combined effect of manufacturing and alignment inaccuracies on the entire system. Monte Carlo analysis provides a statistical

view of the probability of achieving the desired performance and helps identify the most realistic tolerance limits.

In the optical system represented in Figure (5), manufacturing and alignment tolerances are applied to the optical surfaces of M1, M2, L1, L2, and L3. Each optical surface must be analyzed to ensure that the assigned tolerances are tight enough to guarantee the required performance but wide enough to be achievable and maintainable in practice.
The analysis of the telescope tolerances will be divided into two distinct phases to ensure a clearer and more detailed understanding of its performance. Initially, the telescope's performance will be evaluated without the Solar Filter (SF), allowing for a deep study of the fundamental tolerances of the primary optical system. Subsequently, a configuration that includes the Solar Filter will be analyzed. This step-by-step approach has been adopted to simplify the analytical process, avoiding the relative additional complexity introduced by the solar filter in the initial phase of the study. Through this tolerance analysis, it is possible to optimize the telescope design, balancing image quality with production feasibility and costs, while ensuring that the optical system meets the requirements of the space mission. At the end of the tolerance analysis campaign, results and guidelines are obtained on how to manufacture the optics and how to conduct the assembly and alignment process.

5.1 Criterion: RMS Wavefront error

According to REQ 9 (Table (1)), the Root Mean Square (RMS) Wavefront Error has been chosen as the criterion to evaluate the performance of the telescope: this requirement imposes that the system has RMS WFE less than 80 nm. Therefore, this parameter will be used to evaluate the performance and quality of a telescope configuration perturbed by tolerances.
During simulations, multiple telescope configurations deviating from the nominal will be generated. The RMS WFE will be used as the evaluation criterion to determine whether a configuration is acceptable or not.
Using OpticStudio software and ray tracing analysis, the nominal value of RMS WFE can be calculated:

$$\text{RMS\_WFE\_nominal} = 0.022\lambda = 34 \text{ nm}$$

It is expected that configurations perturbed by tolerances, RMS WFE values greater than 34 nm will be obtained, indicating a degradation in the instrument's performance.

5.2 Compensators

A compensator is an element or a set of parameters that can be adjusted to compensate for errors or deviations caused by manufacturing and alignment tolerances in a configuration. These compensators help maintain the optical performance of the system within specified limits. During multiple simulations in the analysis, the compensator's value changes each time to mitigate the errors caused by tolerance perturbations.
In particular, compensators can include:

- **Position and distance of optical elements:** Small adjustments or displacements of the position of lenses, mirrors, or other optical components.
- **Orientation of optical elements:** Adjustments to the tilt or rotation angles of optical elements.
- **Curvature of optical surfaces:** Adjustments to the curvatures of lenses or mirrors, if possible.

The use of compensators allows optimizing the performance of the optical system even in the presence of imperfections or variations due to production and assembly. In OpticStudio, these parameters are defined and adjusted during tolerance analysis to ensure the optical system functions correctly under the intended operating conditions. The parameters intended for use as compensators must be concretely foreseen in the instrument design and are adjusted during the instrument alignment phase.

- Initially, only one compensator was used on the L3 - Sensor distance (Back Focal Distance - BFD) to meet the requirement *"REQ 4 (Table 1): The distance between the last vertex of lens L3 and the Exit Pupil position shall be greater than 68 mm and not greater than 80 mm."* It was found that, being an afocal system, this compensator could not significantly correct the errors due to tolerances: shifting the exit pupil parallel to a collimated beam does not change the performance parameters. In particular, it could not compensate for the tolerances on the curvature radius of mirrors M1 and M2, which were very significant (Worst Offenders) and compromised the performance. The COMP_BFD proved to be ineffective but was still kept in the analysis as it provided minor improvements (in the order of 2 - 4 nanometers) on the RMS WFE error of the Monte Carlo average.
  The compensator parameter has therefore been set to a range of +12.0/-0.0 mm. Since the exact position of the exit pupil is not known and will be defined once the telescope

is integrated, a wide range of values is being used. When the exact position of the sensor (and the exit pupil) is determined, the value of this compensator will also be specified.

- Alongside COMP_BFD, the distance between M2 and the Eyepiece formed by L1-L2-L3 (COMP_EYE) was used as a compensator. Simulations showed that COMP_EYE could mitigate most tolerances, achieving excellent RMS WFE results. The value of COMP_EYE = +/- 1.5mm was found to be sufficient (3 mm total range).
- No other compensator was considered, as COMP_EYE was sufficient.

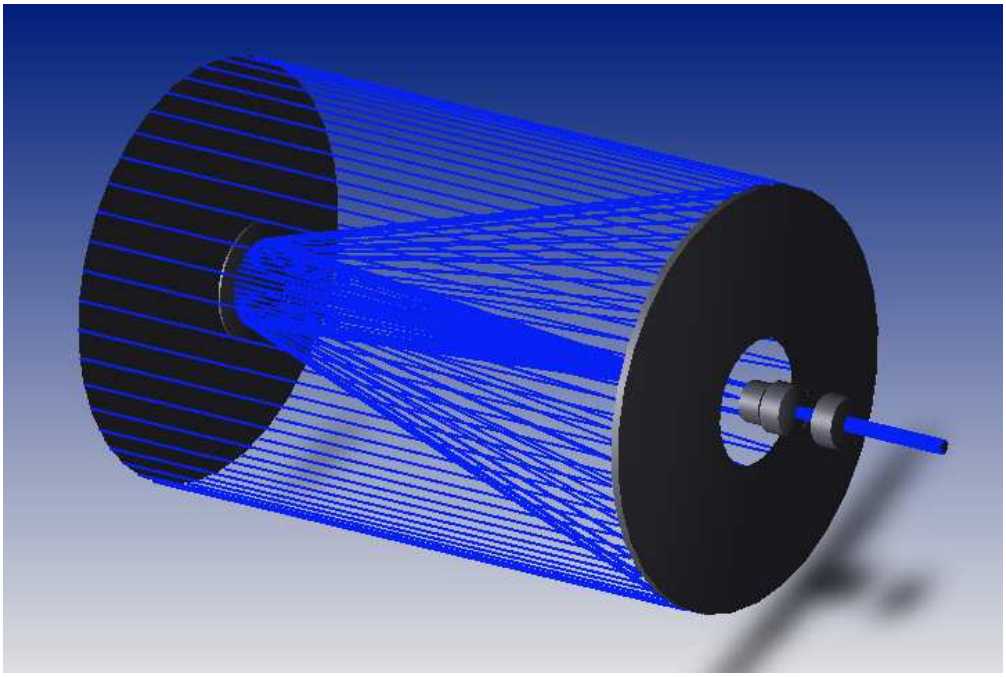

Figure 10: 3D model View of Spock 250 - OpticStudio

5.3 Sensitivity Direct Analysis

Sensitivity analysis is an essential process in optical engineering used to evaluate how individual tolerances impact the overall system performance. By defining the RMS wavefront error (WFE) as the merit function for system performance, this analysis assesses the effect of each tolerance individually on the merit function. This method identifies parameters that are highly sensitive to specific errors, such as variations in surface curvature radii or decenters, allowing engineers to highlight critical areas that require tighter control. It is therefore possible to identify the parameters that most degrade the wavefront error by compiling a list of the so-called "Worst offenders". Additionally, sensitivity analysis is valuable in determining the optimal number of compensators needed for required adjustments. For tolerancing criteria, the defined merit function incorporates the RMS WFE relative to the centroid, adding boundary constraints on the compensators to ensure precise adjustments. This rigorous approach helps optimize the design and maintain high performance standards despite manufacturing and alignment deviations.

5.4 Monte Carlo Analysis

To evaluate the impact of tolerances on Wavefront Error, a Monte Carlo simulation is mandatory. This simulation generates a series of random configurations that comply to the specified tolerances with a normal distribution. In essence, an optical system is created with parameters slightly deviating from their nominal values according to the tolerances. Each parameter is considered to follow a normal distribution, making the simulation a realistic representation of expected performance since all applicable tolerances are simultaneously considered. During the Monte Carlo simulation, numerous iterations are conducted to explore the potential variations in system performance. At the conclusion of these simulations, it is crucial to analyze various statistical outputs, such as the mean and median RMS WFE of the system, the average value of the compensators, scatter diagrams, histograms, and other relevant metrics. These analyses show how well and reliably the optical system works under real manufacturing and alignment conditions. In each Case Study of this thesis, a Monte Carlo simulation involving 400 different configurations was executed to investigate potential performance degradations or variations of the system. The number of simulations was chosen in a reasonable way with an empirical approach, after several attempts, so that they were sufficient to demonstrate the results. This comprehensive tolerance analysis approach was applied to all optical elements, including mirrors and lenses, to ensure a comprehensive eval-

uation. The primary goal of the simulation is to meet the requirement specified in REQ 9 (Table (1)), which needs that the RMS WFE should remain below 80 nm for as many simulations as possible. By applying this tolerance analysis technique, the optical system's design can be optimized to balance performance with practical manufacturing and alignment capabilities, ensuring that the telescope meets its stringent performance criteria.

5.5 OpticStudio - Zemax

This paragraph explains how to set up the ray tracing software OpticStudio - Zemax, allowing other users to repeat the simulations. It is notable that all analyses, including both the Monte Carlo simulation and the sensitivity analysis, were performed on a standard laptop. No high-performance computers, servers, or additional computational resources were required.

5.5.1 General software Set Up

To study the performance of the telescope and conduct tolerance analyses, Ansys OpticStudio Zemax software licensed by the University of Padua was chosen. It is a commercial advanced raytracing software for the design and analysis of optical systems. It allows accurate simulation of light through lenses, mirrors, and other components, providing tools for optimization and performance analysis. Used in several sectors, including the photographic industry, telecommunications industry, and aerospace, it supports both sequential and non-sequential models, facilitating the design of complex systems and the study of tolerance analysis.
Below there are the settings to be configured in the software for the correct study of the instrument. For all other settings, refer to the default setup.
Since Spock 250 is an afocal instrument, the software was configured to correctly compute the data. Following settings are essential:

- Enable the *"AFOCAL IMAGE SPACE"* option: *"System Explorer / Aperture / Afocal Image Space"*; This is necessary to study an afocal system and to correctly calculate the RMS WFE. For further information, refer to the software's *"OpticStudio User Manual"*;
- Ensure that the *"EXIT PUPIL"* is set as the reference in the calculation of the Optical Path Difference and consequently the RMS WFE. *"System Explorer / Advanced / Reference Opd"*.

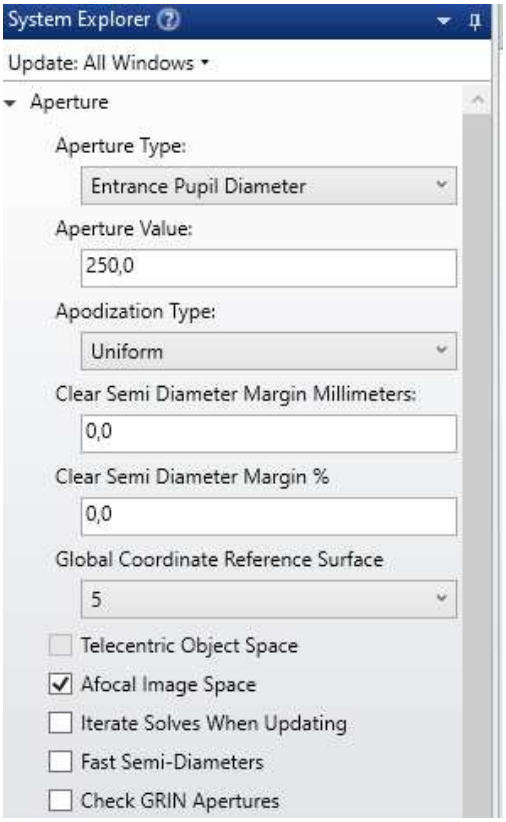

Figure 11: Software Set Up configuration - OpticStudio

Additionally, note the following settings for field, aperture and wavelength:

- Field: X Angle (0°); Y angle (0°); Weight 1.000;
- Aperture: 250.0 mm;
- Wavelength = 1550 nm;

5.5.2 Tolerancing software set up

The tolerance analysis settings are specified in the "Tolerancing" section. It is notable that RMS wavefront is chosen as Criterion, Damped Least Squares (DLS) is selected as the compensator optimization algorithm, 400 simulations are performed, and a normal distribution is used for the tolerance parameters.

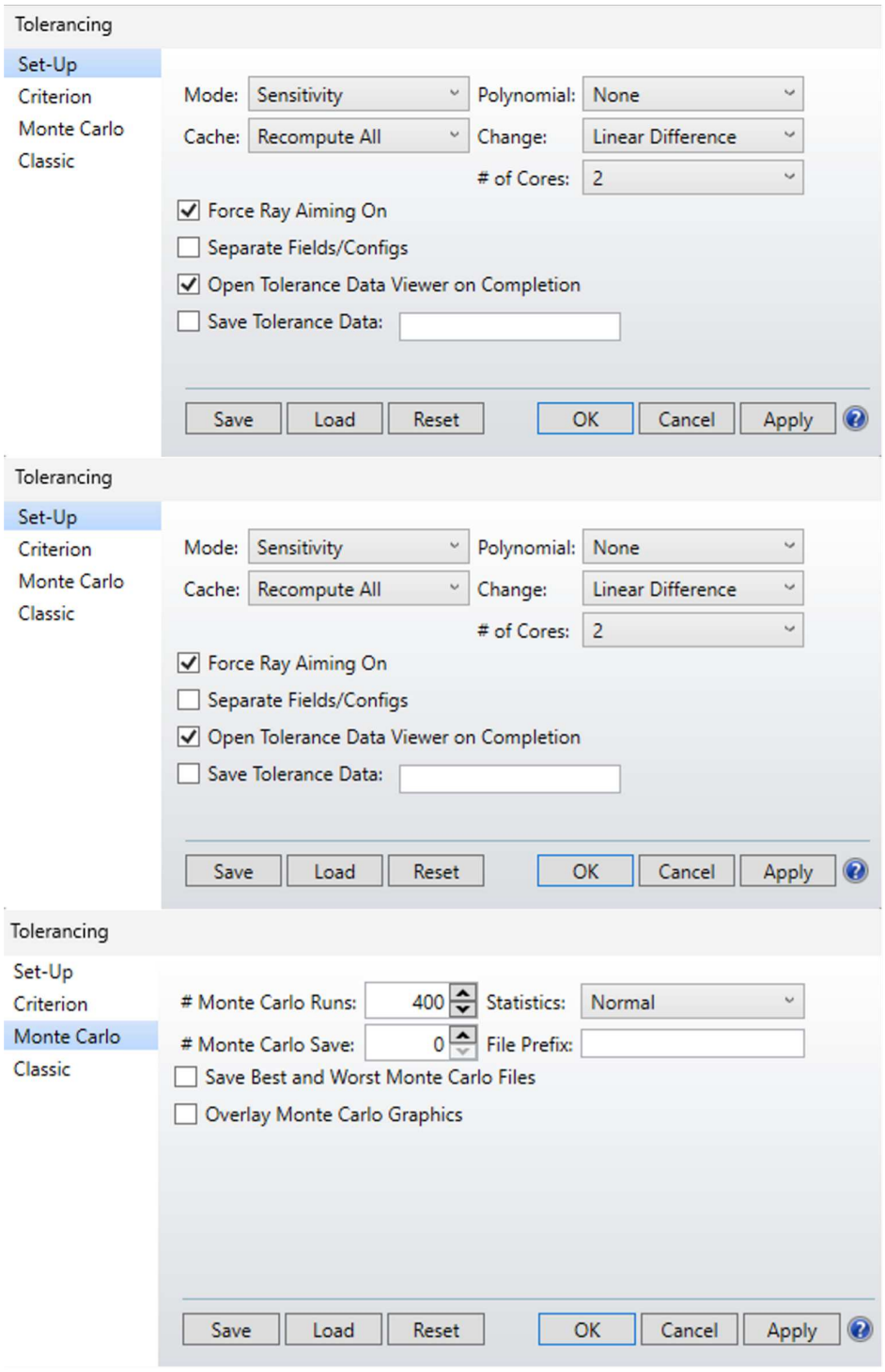

Figure 12: Tolerancing Set Up configuration - OpticStudio

6 Spock Ø250mm Telescope: Tolerance Analysis

Initially, very restrictive alignment and manufacturing tolerances were set to obtain a preliminary idea of the telescope's performance. Subsequently, the tolerance values were gradually relaxed, analyzing how the optical system responded to different tolerance configurations. This process allowed for the identification of "worst offenders," i.e., the parameters that most significantly degrade the telescope's performance. Consequently, only the tolerances that had a significant impact on the system were tightened, ensuring an optimal combination of performance and feasibility.
In parallel, an in-depth study on the optimal range of compensator parameter values was conducted. Through numerous iterations, the system's behavior was observed as the compensators varied. Finally, the compensator ranges were chosen based on feasibility considerations and performance analysis.
Four case studies are presented to demonstrate how the optical system's performance is affected by tightening or relaxing tolerance values. The illustrated cases show only the most relevant analysis data, including the "worst offenders," the mean and median of the Monte Carlo simulations, scatter diagrams, histograms, box plots, and some results related to the compensators.
The analyzed cases through Monte Carlo simulations are illustrated below:

- **Case 1**: Optimal tolerances, a compromise between telescope performance and less restrictive tolerances.
  - Monte Carlo average for 400 simulations: RMS_WFE_mean = 40.62 nm
- **Case 2**: More relaxed tolerances, demonstrating that some parameters must necessarily be tightened.
  - Monte Carlo average for 400 simulations: RMS_WFE_mean = 70.41 nm
- **Case 3** (3.1, 3.2): Tolerances similar to "Case 1" except for the tolerance on the curvature radius of M1, which is relaxed. Additionally, the range of the COMP_EYE is varied each time to study its effect. These cases are used to investigate how the curvature radius of M1 influences the telescope's performance and how it requires a suitable compensator.
  - Case 3.2 - Monte Carlo average for 400 simulations: RMS_WFE_mean = 54.85 nm

- **Case 4**: The solar filter has been analyzed: after being added to the optical configuration, its impact on the system was studied.
  - Monte Carlo average for 400 simulations: RMS_WFE_mean = 41.02 nm

6.1 Case 1

6.1.1 Tolerances

The following "Case 1" represents an excellent trade-off between performance and manufacturing/alignment costs. The tolerances, which are not too stringent and can potentially be further tightened, ensure a performance that comfortably meets the Wave Front Error requirement (< 80 nm). At the same time, they do not present critical issues during the fabrication of optical surfaces or alignment. It should be noted that only the curvature radius of the mirrors and the positioning and alignment of the secondary mirror are the parameters that require greater precision.
Compensators are sets as follows:

- The COMP_EYE compensator is set to +/- 1.5 mm.
- The COMP_BFD compensator is set to position the exit pupil between 68 mm and 80 mm from lens L3 (REQ 4 - Table (1)).

Below there is the Tolerance Table (4). This table is only indicative; for the complete list of tolerances, refer to the "Tolerance Data" (Table (6)).

	PARAMETER	TOLERANCE
M1,M2	Δ Radius Curvature	$\pm 0.01\%$ (high precision)
	Δz	± 0.1 mm
	Decenter	± 0.05 mm
	Tilt	$\pm 0.05°$
	Surface Irregularity	$\pm 0.1\lambda$
		($\lambda = 633$ nm)
L1,L2,L3	Δ Radius Curvature	$\pm 0.1\%$ (precision)
	Δz	± 0.1 mm
	Decenter	± 0.1 mm
	Tilt	$\pm 0.1°$
	Surf Irr	$\pm 0.1\lambda$ PTV
		($\lambda = 633$ nm)
COMPENSATOR	Comp EYE	± 1.5 mm
	Comp BFD	$68\,\text{mm} < z < 80\,\text{mm}$

Table 4: Manufacturing and alignment Tolerance of "Case 1" configuration

"High precision" and "Precision" refer to manufacturing classes. The tightest tolerances are highlighted in red. As can be seen, the tolerances on the curvature radius of mirrors M1 and M2 are given as a percentage of the curvature radius of the mirrors and are set to $\pm 0.01\%$. (See Table (2) for mirror characteristics). Δz is the positional tolerance of the element along the optical axis of the telescope; tilt and decenter refer to alignment tolerances and are set to ± 0.05 mm and $\pm 0.05°$ for mirror M2 (which requires greater control) and ± 0.1 mm and $\pm 0.1°$ for lens alignment.

It should also be noted that the reference surface, from which the alignment campaign is then carried out, is mirror M1. Therefore, there are no alignment tolerances on this surface. The surface irregularity tolerance is set at ± 0.1 λ (PTV) with a test wavelength of 633 nm (He-Ne laser wavelength).

6.1.2 Monte Carlo Simulation

400 Monte Carlo simulations are performed (see "Tolerance software setup" for details 5.5.2). It has been chosen to use 400 simulations as this number is sufficient to obtain representative results for the problem. The RMS Wave Front Error values obtained from the Monte Carlo simulation are shown in Table (22) below.

Case 1	Nominal	Mean	Median
RMS WFE [nm]	14,70	40,62	35,75

Table 5: 400 Monte Carlo simulations. Nominal, Mean, Median RMS Wave Front Error of "Case 1"

The "Nominal" RMS WFE corresponds to the value calculated by the program in the nominal case without consider the effects of tolerances. "Mean" and "Median" RMS WFE represent the mean and median of all 400 Monte Carlo simulations.
Note: The nominal value of 14.70 nm is obtained with the adjustment of COMP_EYE. Without the compensator, the optical system has a nominal error of $0,022\lambda = 34.59$ nm ($\lambda = 1550$ nm). This suggests that the initial configuration, without a compensator, is not the optimal one with minimum RMS WFE. However, the problem can be overcome by applying COMP_EYE and then calibrating the position of the eyepiece during the alignment campaign.
400 Monte Carlo simulations are performed using OpticStudio software. Following that, several graphs were produced for the analysis and interpretation of the results.

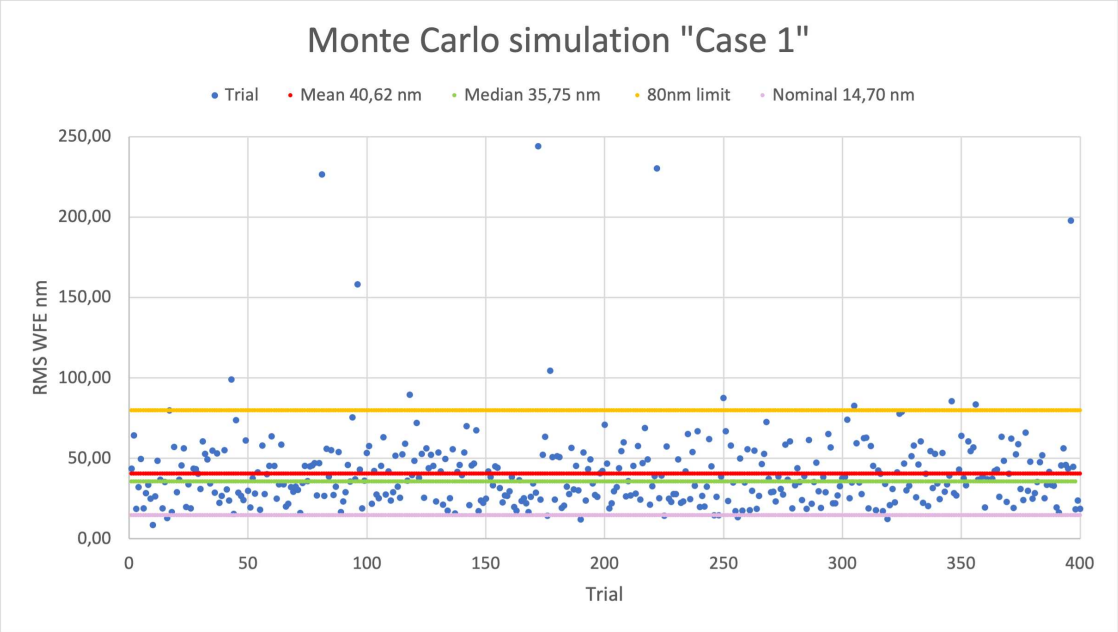

Figure 13: 400 Monte Carlo simulations - “Case 1” - Scatter Diagram

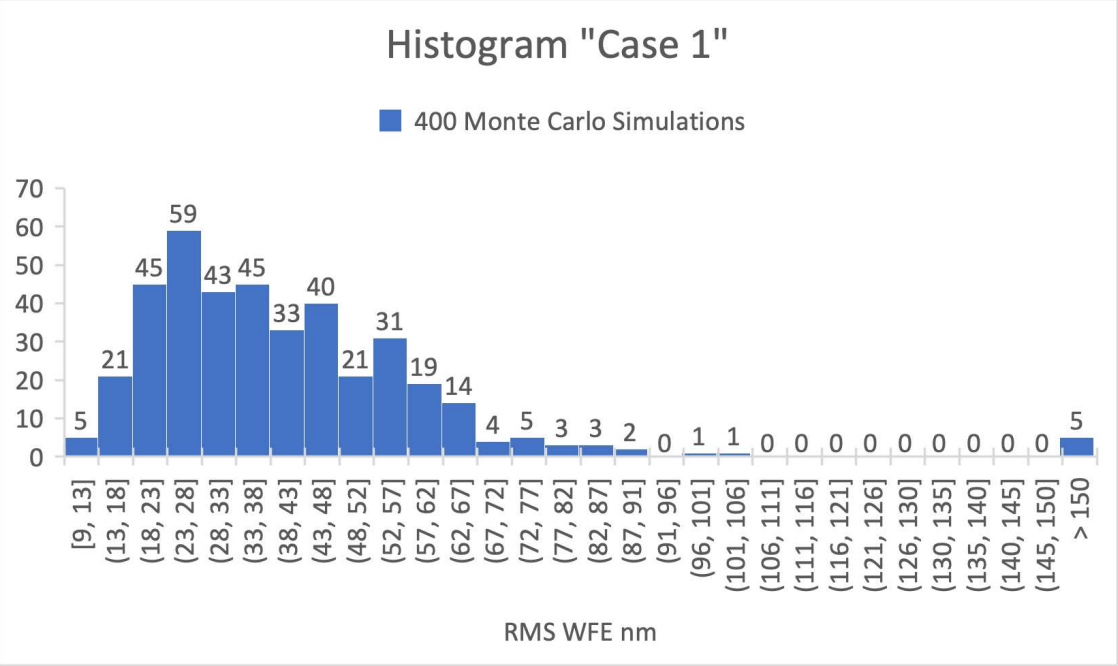

Figure 14: 400 Monte Carlo simulations - “Case 1” - Histogram

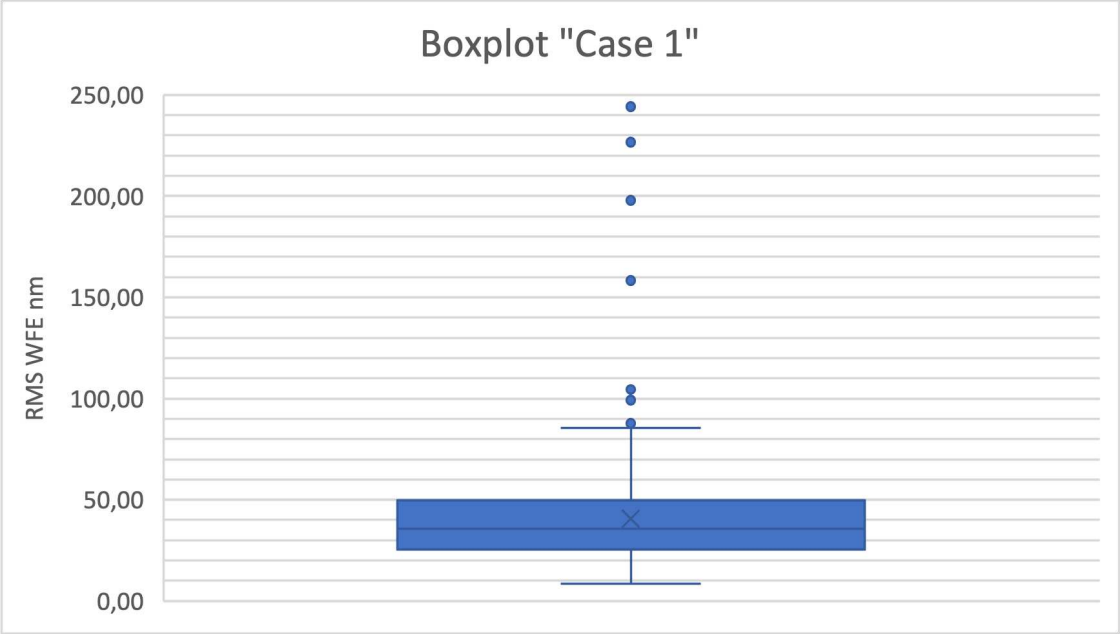

Figure 15: 400 Monte Carlo simulations - “Case 1” - Boxplot

Scatter Diagram The chart (Figure(13)) shows the distribution of WFE of the 400 simulations. The Mean (40.62 nm), the Median (35.75 nm), and the nominal value (14.70 nm) are highlighted. Some outliers can be observed that deviate significantly from the other results. Investigating these and analyzing the individual simulations, it is noted that the combination of the misalignment of M2 (Tilt and Decenter) and the distance between M1 and M2 produces an amplification of the wavefront error. This is supported by the “Sensitivity Analysis” which shows that these parameters are the Worst Offenders (see Table (7)). 96.5% of the results meet the upper limit of 80 nm; the data are concentrated around the Mean 40.62 nm. The nominal value 14.70 nm can be considered the lower limit of the telescope’s performance except for some cases where the WFE reaches 10 nm (5 simulations).

Histogram The histogram (Figure (28)) shows the distribution of RMS WFE. We can see that most values are concentrated between 9 nm and 67 nm, with a peak around 25 nm. There are five simulations that produced RMS WFE values greater than 150 nm, indicating significantly higher optical aberration than the other simulations. The cause is due to the simultaneous combination of several worst offenders. The shape of the histogram is asymmetrical, with a longer tail towards higher RMS WFE values. The graph shows that the configuration of “Case 1” is an excellent result that meets the requirements.

Boxplot The boxplot (Figure (15)) shows the results of 400 simulations, helping to interpret the results from another perspective. The Median RMS WFE is 35.75 nm (dark horizontal line within the box), with the interquartile range (IQR) varying between 25 nm and 50 nm, indicating that 50% of the data is within this range. The cross indicates the mean value. The "whiskers" (blue horizontal segments in the graph) extend approximately from 10 nm to 85 nm, showing the range of data variability excluding the outliers (98% of the data is within this range). This indicates a stable central distribution but with some exceptional cases.

Table 6: Tolerance Data "Case 1" - all Manufacturing and Alignment Tolerances data of every element/surface - Zemax OpticStudio

Type	Int1	Int2	Nominal	Min	Max	Comment
COMP	4	0	350	-1.5	1.5	COMP_EYE
COMP	10	0	68.007	0	12	COMP_BFD
TWAV				0.633		Default test wavelength.
TRAD	3	1	-875.001	-1.00E-02	1.00E-02	Default radius tolerances.
TRAD	4	1	-235.637	-1.00E-02	1.00E-02	
TRAD	5	1	-28.981	-0.1	0.1	
TRAD	6	1	164.385	-0.1	0.1	
TRAD	7	1	-334.512	-0.1	0.1	
TRAD	8	1	-38.401	-0.1	0.1	
TRAD	9	1	132.653	-0.1	0.1	
TRAD	10	1	-141.612	-0.1	0.1	
TTHI	3	4	-350	-0.1	0.1	Default thickness tolerances.
TTHI	4	6	350	-0.1	0.1	
TTHI	5	6	12.056	-0.1	0.1	
TTHI	6	8	3.74	-0.1	0.1	
TTHI	7	8	16.125	-0.1	0.1	
TTHI	8	10	19.555	-0.1	0.1	
TTHI	9	10	16.036	-0.1	0.1	
TEDX	4	4	0	-0.05	0.05	Default element dec/tilt tolerances 4-4.
TEDY	4	4	0	-0.05	0.05	
TETX	4	4	0	-0.05	0.05	
TETY	4	4	0	-0.05	0.05	
TEDX	5	6	0	-0.1	0.1	Default element dec/tilt tolerances 5-6.
TEDY	5	6	0	-0.1	0.1	
TETX	5	6	0	-0.1	0.1	
TETY	5	6	0	-0.1	0.1	
TEDX	7	8	0	-0.1	0.1	Default element dec/tilt tolerances 7-8.
TEDY	7	8	0	-0.1	0.1	
TETX	7	8	0	-0.1	0.1	
TETY	7	8	0	-0.1	0.1	

Type	Int1	Int2	Nominal	Min	Max	Comment
TEDX	9	10	0	-0.1	0.1	Default element dec/tilt tolerances 9-10.
TEDY	9	10	0	-0.1	0.1	
TETX	9	10	0	-0.1	0.1	
TETY	9	10	0	-0.1	0.1	
TSDX	5		0	-0.1	0.1	Default surface dec/tilt tolerances 5.
TSDY	5		0	-0.1	0.1	
TSTX	5		0	-0.1	0.1	
TSTY	5		0	-0.1	0.1	
TSDX	6		0	-0.1	0.1	Default surface dec/tilt tolerances 6.
TSDY	6		0	-0.1	0.1	
TSTX	6		0	-0.1	0.1	
TSTY	6		0	-0.1	0.1	
TSDX	7		0	-0.1	0.1	Default surface dec/tilt tolerances 7.
TSDY	7		0	-0.1	0.1	
TSTX	7		0	-0.1	0.1	
TSTY	7		0	-0.1	0.1	
TSDX	8		0	-0.1	0.1	Default surface dec/tilt tolerances 8.
TSDY	8		0	-0.1	0.1	
TSTX	8		0	-0.1	0.1	
TSTY	8		0	-0.1	0.1	
TSDX	9		0	-0.1	0.1	Default surface dec/tilt tolerances 9.
TSDY	9		0	-0.1	0.1	
TSTX	9		0	-0.1	0.1	
TSTY	9		0	-0.1	0.1	
TSDX	10		0	-0.1	0.1	Default surface dec/tilt tolerances 10.
TSDY	10		0	-0.1	0.1	
TSTX	10		0	-0.1	0.017	
TSTY	10		0	-0.1	0.017	
TIRR	3		0	-0.1	0.1	Default irregularity tolerances.
TIRR	4		0	-0.1	0.1	
TIRR	5		0	-0.1	0.1	
TIRR	6		0	-0.1	0.1	

Type	Int1	Int2	Nominal	Min	Max	Comment
TIRR	7		0	-0.1	0.1	
TIRR	8		0	-0.1	0.1	
TIRR	9		0	-0.1	0.1	
TIRR	10		0	-0.1	0.1	

6.1.3 Tolerance data Editor

Above is shown the setup of the "Tolerance Data Editor" in OpticStudio (Table 6), where all the tolerances for each individual element/surface can be found in order to reproduce the simulation. For more information on the individual "Operands," please consult the "OpticStudio User Manual." These are the tolerances resulting from the conducted analysis, and they are considered as the final results of the tolerance analysis for 'Case 1'.

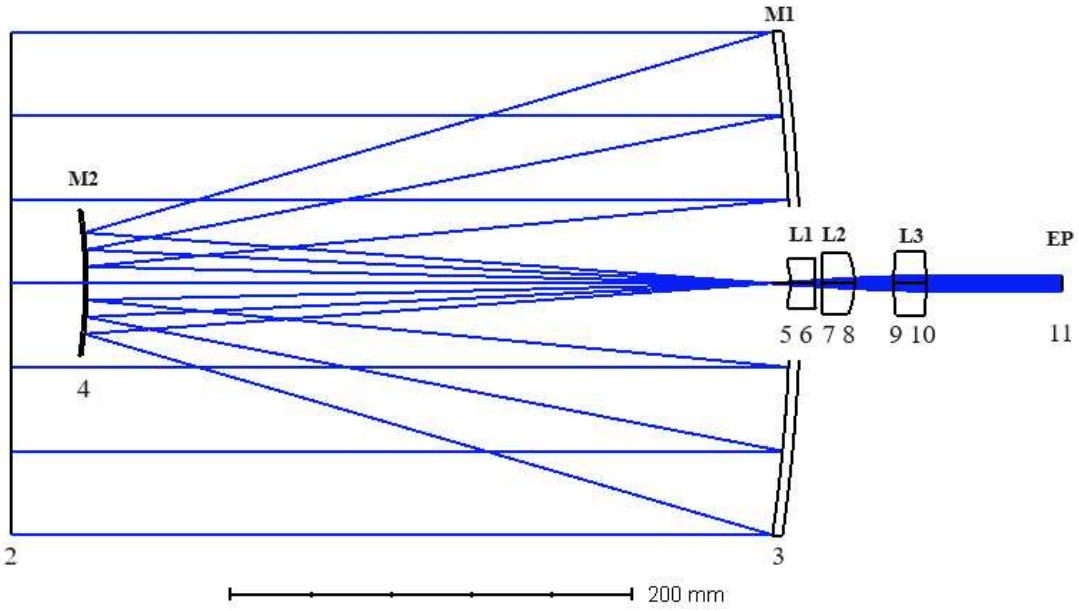

Figure 16: Optical Design - the numbers represent the surface's number in OpticStudio

6.1.4 Worst offenders

From the Sensitivity Analysis, the *Worst Offenders* have been identified: these are the tolerances that contribute most to wavefront errors (Table (7)). The column "Change nm" refers to the difference between the nominal RMS WFE value (14,40 nm) and the value assumed in the nominal configuration with only the indicated tolerance change.

Type	Surface	Tolerance	WFE nm	Change nm
TETX	4	-0.05	50.26	35.56
TETX	4	+0.05	50.26	35.56
TETY	4	+0.05	50.26	35.56
TETY	4	-0.05	50.26	35.56
TEDY	4	+0.05	37.22	22.52
TEDY	4	-0.05	37.22	22.52
TEDX	4	+0.05	37.22	22.52
TEDX	4	-0.05	37.22	22.52
TTHI	3-4	+0.1	27.28	12.58
TIRR	3	-0.1	18.09	3.39

Table 7: Worst Offenders "Case 1"

- **TETX and TETY** (Tolerance Element Tilt X/Y): $\pm 0.05°$ variations in both X and Y axes result in a significant increase in WFE by 35.55 nm.
- **TEDX and TEDY** (Tolerance Element Decenter X/Y): ± 0.05 mm variations in both X and Y axes increase WFE of 22.5 nm.
- **TTHI** (Tolerance on Thickness): A 0.1 mm variation results in a increase of 12.57 nm in the criterion.
- **TIRR** (Tolerance on surface irregularity PTV): A -0.1λ variation results in a increase of 3.39 nm in the criterion.

These results highlight the parameters that, if optimized, can significantly reduce RMS WFE. In particular, variations in TETX, TETY, TEDX, and TEDY parameters on Mirror M2 (surface 4) have a notable impact, suggesting that the combination of these factors is mainly responsible for the outliers observed in the graphs. Therefore, focusing on optimizing these parameters could lead to significant improvements in telescope performance.

6.1.5 Summary of Monte Carlo simulation "Case 1"

	RMS WFE (nm)	
Nominal	14.70	
Best	8.61	
Worst	244.16	
Mean	40.62	
Median	37.75	
Std Dev		0.0164
COMP_EYE	Thickness [mm]	
Nominal	350.04	
Minimum	348.50	
Maximum	351.50	
Mean	350.02	
Standard Deviation		0.726
COMP_BFD	Thickness [mm]	
Nominal	69.87	
Minimum	68.26	
Maximum	79.92	
Mean	72.76	
Standard Deviation		2.853
RMS WFE Statistics	RMS WFE nm	
90% >	61.35	
80% >	53.58	
50% >	35.75	
20% >	23.97	
10% >	19.39	

Table 8: Summarize of Monte Carlo simulations “Case 1” – OpticStudio

6.1.6 Compensators

The COMP_EYE compensator, in the worst-case simulations, reaches saturation (See Table (8)). This might suggest expanding the range of the COMP_EYE. Later simulations, not reported here, have shown that even doubling the compensator range between -3mm and +3mm does not compensate for the worst results. The value of +/-1.5mm is an optimal and reasonable value obtained after numerous trials. The adjustment of the compensator must be very precise, as it ensures the calibration of the optical system by significantly mitigating the WFE. The COMP_BFD compensator takes on various values during the simulations. Due to its wide range, the software allows it to move freely, never reaching saturation. As previously discussed, this compensator is not very effective for this afocal system. Nevertheless, it is used because it improves the Monte Carlo average performance by 2-4 nm.

6.2 Case 2

The following "Case 2" aims to demonstrate how the stricter Tilt and Decenter tolerances of the M2 mirror, adopted in "Case 1", are crucial for achieving good results. "Case 2" is a configuration where these tolerances have been relaxed. The tolerances for the M2 mirror are:

- In **"Case 1"**:
  - tilt (TETX and TETY) set to ±0.05°;
  - decenter (TEDX and TEDY) set to ±0.05 mm;
- In **"Case 2"**:
  - tilt (TETX and TETY) set to ±0.1°;
  - decenter (TEDX and TEDY) set to ±0.1 mm;

The compensator are set as the previus case as follow:

- The COMP_EYE compensator is set to ±1.5 mm.
- The COMP_BFD compensator is set so that the exit pupil is positioned between 68 mm and 80 mm from lens L3 (REQ 4 - Table (1)).

Below there is the tolerance table (Table 9). For the list of all specific tolerances, refer to the "Tolerance Data" (Table (11)).

	PARAMETER	TOLERANCE
M1,M2	Δ Radius Curvature	$\pm 0.01\%$ (high precision)
	Δz	± 0.1 mm
	Decenter	± 0.1 mm
	Tilt	$\pm 0.1^\circ$
	Surface Irregularity	$\pm 0.1\lambda$
		($\lambda = 633$ nm)
L1,L2,L3	Δ Radius Curvature	$\pm 0.1\%$ (precision)
	Δz	± 0.1 mm
	Decenter	± 0.1 mm
	Tilt	$\pm 0.1^\circ$
	Surf Irr	$\pm 0.1\lambda$ PTV
		($\lambda = 633$ nm)
COMPENSATOR	Comp EYE	± 1.5 mm
	Comp BFD	68 mm $< z <$ 80 mm

Table 9: Manufacturing and alignment Tolerance of "Case 2" configuration

As can be seen in green colour the table, the decenter and tilt tolerances of the M2 mirror are relaxed. It is noted that M1 is used as the reference surface to which alignment tolerances are not applied.
Below there are the RMS Wave Front Error values (Table (10)).

Case 2	Nominal	Mean	Median
RMS WFE [nm]	14,70	72,49	71,31

Table 10: 400 Monte Carlo simulations. Nominal, Mean, Median RMS Wave Front Error of "Case 2"

The "Nominal" RMS WFE corresponds to the value calculated by the program in the nominal

case without consider the effects of tolerances. "Mean" and "Median" RMS WFE represent the mean and median of all 400 Monte Carlo simulations.

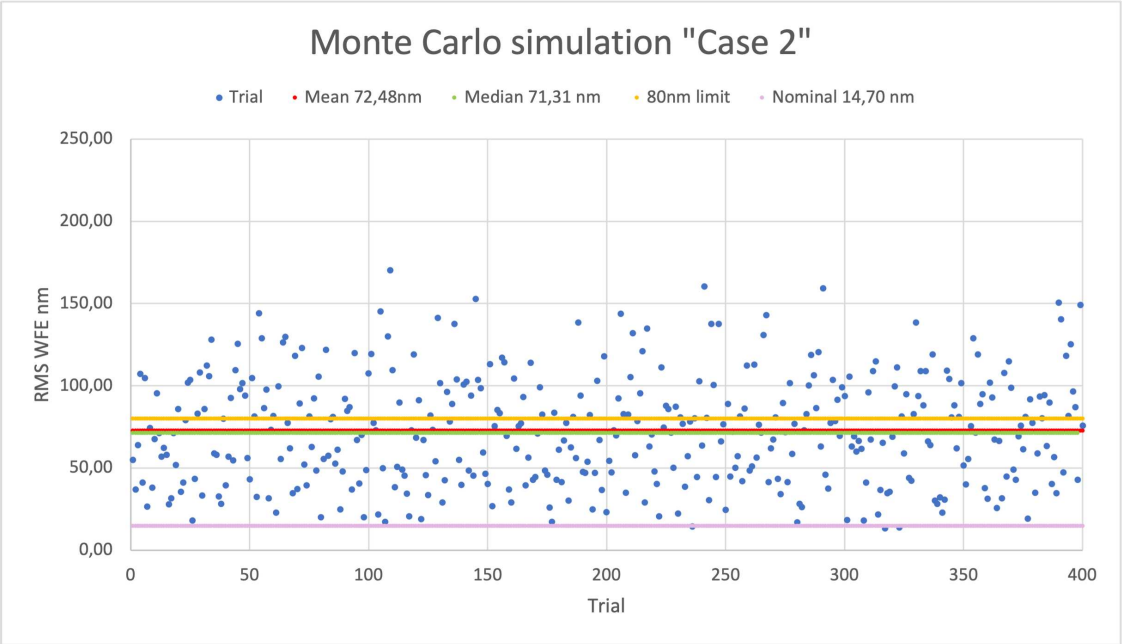

Figure 17: 400 Monte Carlo simulations - “Case 2” - Scatter Diagram

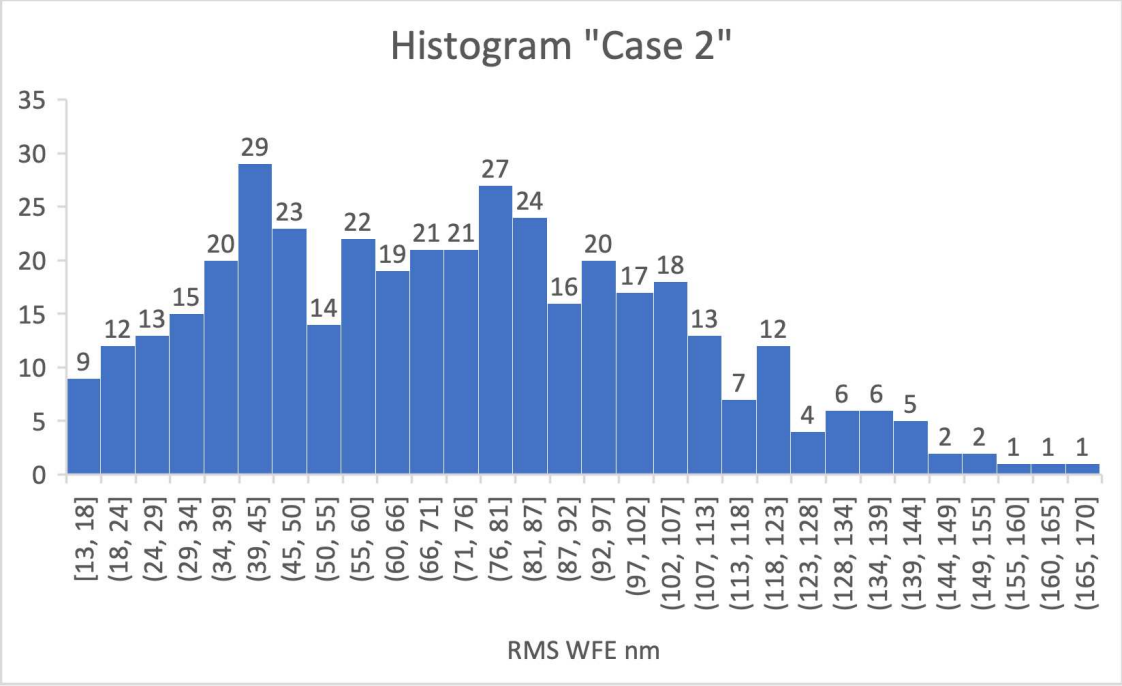

Figure 18: 400 Monte Carlo simulations - “Case 2” - Histogram

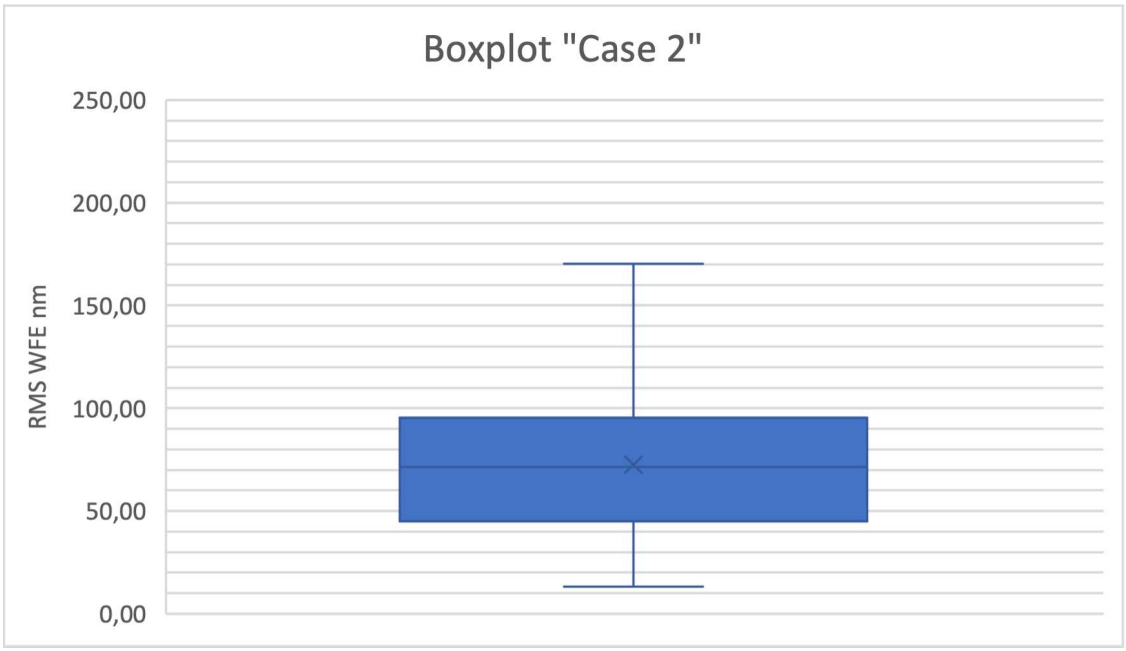

Figure 19: 400 Monte Carlo simulations - “Case 2” - Boxplot

In this case as well, 400 Monte Carlo simulations were performed using OpticStudio with the same settings as in "Case 1". Some charts were then produced for the analysis and interpretation of the results.

Scatter Diagram The graph (Figure (17)) shows the distribution of WFE (Wave Front Error) from the 400 simulations conducted in "Case 2". The average (72.48 nm), nominal value (14.70 nm), and the requirement value of 80 nm are highlighted. The distribution of blue dots indicates the RMS WFE values obtained in each simulation. It can be observed that most values cluster around the average of 72.48 nm (red line), with frequent deviations reaching significantly higher values. This suggests that while many optical configurations fall within acceptable limits, numerous simulations exhibit high WFE errors that do not meet the requirements.
The yellow line represents the maximum limit of 80 nm, highlighting that a considerable number of simulations exceed this threshold, indicating the need for further refinement of the optical system tolerances. Finally, the pink line shows the nominal value of 14.70 nm. This indicates that under ideal conditions, the wavefront error is much lower compared to simulation results, suggesting that variations in tolerances have a significant impact on telescope performance.
In conclusion, the graph emphasizes the importance of stringent tolerance control to ensure

optimal optical performance and minimize telescope wavefront error. It is evident that "Case 1" performs better than "Case 2" and underscores the need to refine certain tolerances.

Histogram The histogram (Figure (18)) represents the distribution of wavefront error (WFE) values obtained from 400 Monte Carlo simulations. The histogram bins, shown on the x-axis, represent intervals of RMS WFE values, while the y-axis indicates the frequency at which RMS WFE values occur within each interval.
It can be observed that the data distribution is slightly asymmetric, with a right-shifted tail. Most RMS WFE values concentrate in the lower intervals, with the peak in the range [76,84] nm, indicating that most simulations produced wavefront errors within this range. This is consistent with the average value of 72.48 nm observed in the previous scatter plot.
The presence of significant values beyond the 80 nm range, as highlighted in the scatter plot, is further confirmed by the histogram. However, the number of occurrences progressively decreases for higher intervals, suggesting that events with extremely high wavefront errors are less frequent but still present.

Boxplot In the boxplot (Figure (19)), the median line within the box indicates the median value of RMS WFE, which is 71.31 nm. The box itself represents the interquartile range (IQR), containing the central 50% of the data. In this case, the IQR extends approximately from 52 nm to 100 nm, showing significant variability in the data. The whiskers of the boxplot extend to the most extreme data points that are not considered outliers. Points outside the whiskers are considered outliers. In this case, there is one outlier above 160 nm. From the scatter plot, this result can be interpreted not as a true outlier but as a simulation particularly affected by WFE.
The boxplot confirms the distribution observed in the previous histogram, showing a higher concentration of data in the range between 52 nm and 100 nm.

Type	Int1	Int2	Nominal	Min	Max	Comment
COMP	4	0	350	-1.5	1.5	COMP_EYE
COMP	10	0	68.007	0	12	COMP_BFD
TWAV				0.633		Default test wavelength.
TRAD	3	1	-875.001	-1.00E-02	1.00E-02	Default radius tolerances.
TRAD	4	1	-235.637	-1.00E-02	1.00E-02	
TRAD	5	1	-28.981	-0.1	0.1	
TRAD	6	1	164.385	-0.1	0.1	
TRAD	7	1	-334.512	-0.1	0.1	
TRAD	8	1	-38.401	-0.1	0.1	
TRAD	9	1	132.653	-0.1	0.1	
TRAD	10	1	-141.612	-0.1	0.1	
TTHI	3	4	-350	-0.1	0.1	Default thickness tolerances.
TTHI	4	6	350	-0.1	0.1	
TTHI	5	6	12.056	-0.1	0.1	
TTHI	6	8	3.74	-0.1	0.1	
TTHI	7	8	16.125	-0.1	0.1	
TTHI	8	10	19.555	-0.1	0.1	
TTHI	9	10	16.036	-0.1	0.1	
TEDX	4	4	0	-0.1	0.1	Default element dec/tilt tolerances 4-4.
TEDY	4	4	0	-0.1	0.1	
TETX	4	4	0	-0.1	0.1	
TETY	4	4	0	-0.1	0.1	
TEDX	5	6	0	-0.1	0.1	Default element dec/tilt tolerances 5-6.
...	...	...	...	...	...	...

Table 11: Tolerance Data “Case 2” - few Manufacturing and Alignment Tolerances - OpticStudio

6.2.1 Tolerance Data Editor

Above is shown the setup of the "Tolerance Data Editor" in OpticStudio where you can find some of the tolerances for the telescope elements (Table (11)). For all other tolerances, refer to Table 6 of "Case 1". In red, the decenter and tilt tolerances of the M2 mirror (surface 4) have been relaxed to 0.1 mm and 0.1°, respectively. For more information on individual

operands, please refer to the "User Manual".

6.2.2 Worst offenders

Type	Surface	Tolerance	WFE nm	Change nm
TETX	4	-0.1	97.38	82.67
TETX	4	+0.1	97.38	82.67
TETY	4	+0.1	97.38	82.67
TETY	4	-0.1	97.38	82.67
TEDY	4	-0.1	69.95	55.25
TEDY	4	+0.1	69.95	55.25
TEDX	4	-0.1	69.95	55.25
TEDX	4	+0.1	69.95	55.25
TTHI	3-4	+0.1	27.28	12.58
TIRR	3	-0.1	18.09	3.39

Table 12: Worst Offenders "Case 2"

From the analyses conducted, the *worst offenders* contributing most to wavefront errors have been identified (**Table 9**). Here is a summary of the parameters and their respective changes:

- **TETX and TETY** (Tolerance Element Tilt X/Y): Variations of $\pm 0.1°$ in both X and Y axes lead to significant changes in WFE, with an increase of 82 nm.
- **TEDX and TEDY** (Tolerance Element Decenter X/Y): Variations of ± 0.1 mm in both X and Y axes result in an increase of 55 nm.
- **TTHI** (Tolerance on Thickness): A variation of 0.1 mm results in an increase in WFE by 12 nm.
- **TIRR** (Tolerance on surface irregularity PTV): A variation of -0.1 λ increase WFE by 3 nm.

These results highlight parameters that, if optimized, can significantly reduce RMS WFE. Specifically, variations in TETX, TETY, TEDX, and TEDY parameters have a notable impact. Restricting these tolerances could greatly enhance performance. In "Case 1", these tilt and decenter tolerances were narrowed down to 0.05° and 0.05 mm, respectively, which were found to be the most critical.

6.2.3 Summary of Monte Carlo simulation "Case 2"

	RMS WFE (nm)	
Nominal	14.70	
Best	13.22	
Worst	170.3	
Mean	72.49	
Median	71.31	
Std Dev		0.0212
COMP_EYE	Thickness [mm]	
Nominal	350,04	
Minimum	348,50	
Maximum	351,50	
Mean	350,09	
Standard Deviation		0,712
COMP_BFD	Thickness [mm]	
Nominal	69,87	
Minimum	68,15	
Maximum	79,95	
Mean	72,76	
Standard Deviation		3,120
RMS WFE Statistics	RMS WFE nm	
90% >	118.02	
80% >	101.73	
50% >	71.31	
20% >	41.12	
10% >	31.02	

Table 13: Summarize of Monte Carlo simulations “Case 2” – OpticStudio

6.2.4 Compensators

In this case as well, considerations regarding the compensator are analogous to "Case 1". The COMP_EYE compensator, in the worst simulations, saturates. However, increasing its range would still not effectively compensate for the WFE (Table 13). This statement is supported by additional simulations, not reported here.

6.3 Case 3

The following "Case 3.1" aims to demonstrate how relaxing the tolerance on the radius of curvature of M1 influences the results. Compared to "Case 1", tolerances on all optical elements except the curvature radius of M1 remain unchanged. This tolerance (ΔRadius Curvature) is expressed as a percentage of the radius of curvature:

- In **"Case 1"**:
  - TRAD_M1 = ±0.01%
  - Radius_of_Curvature_M1 = 875.001 mm
  - ΔRadius Curvature = 875.001 mm × 0.01% = 0.0875 mm or ±0.0875 mm
- In **"Case 3.1"**:
  - TRAD_M1 = ±0.05%
  - Radius_of_Curvature_M1 = 875.001 mm
  - ΔRadius Curvature = 875.001 mm × 0.05% = 0.4375 mm or ±0.4375 mm

  The COMP_EYE is set to ±1.5 mm.

	PARAMETER	TOLERANCE
M1	Δ Radius Curvature	$\pm 0.05\%$
M2	Δ Radius Curvature	$\pm 0.01\%$
	Δz	± 0.1 mm
	Decenter	± 0.05 mm
	Tilt	$\pm 0.05°$
	Surface Irregularity	$\pm 0.1\lambda$
		($\lambda = 633$ nm)
L1,L2,L3	Δ Radius Curvature	$\pm 0.1\%$ (precision)
	Δz	± 0.1 mm
	Decenter	± 0.1 mm
	Tilt	$\pm 0.1°$
	Surf Irr	$\pm 0.1\lambda$ PTV
		($\lambda = 633$ nm)
COMPENSATOR	Comp EYE	± 1.5 mm
	Comp BFD	$68\,\text{mm} < z < 80\,\text{mm}$

Table 14: Manufacturing and alignment Tolerance of "Case 3.1" configuration

Below there are the values of RMS Wave Front Error (Table 15).

Case 3.1	Nominal	Mean	Median
RMS WFE [nm]	14,70	226,86	71,31

Table 15: 400 Monte Carlo simulations. Nominal, Mean, Median RMS Wave Front Error of "Case 3.1"

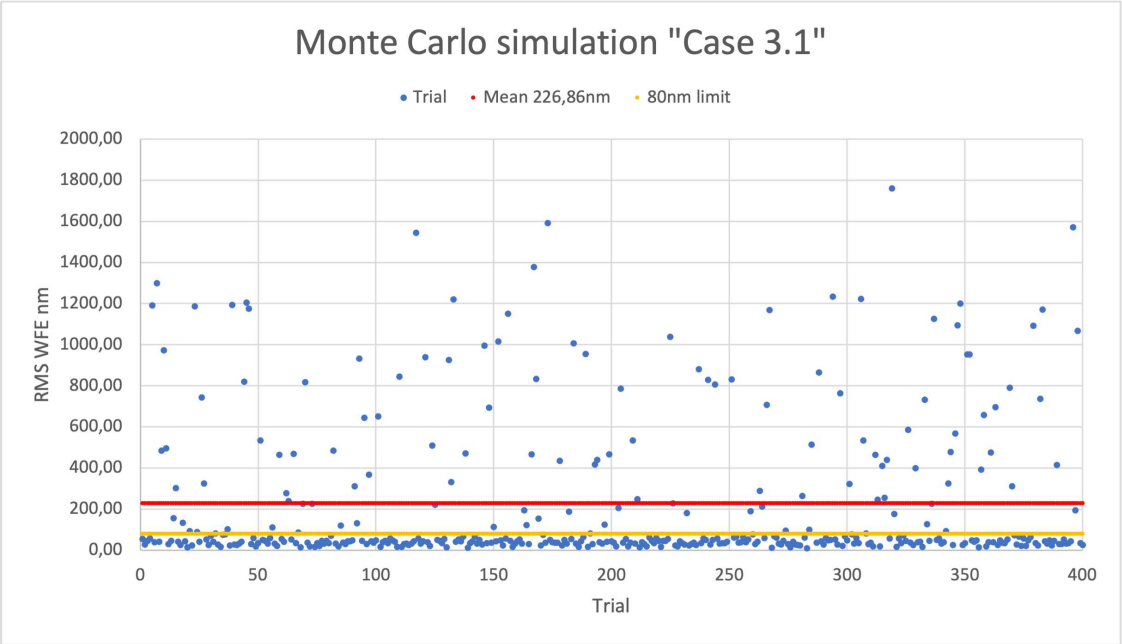

Figure 20: 400 Monte Carlo simulations - “Case 3.1” - Scatter Diagram

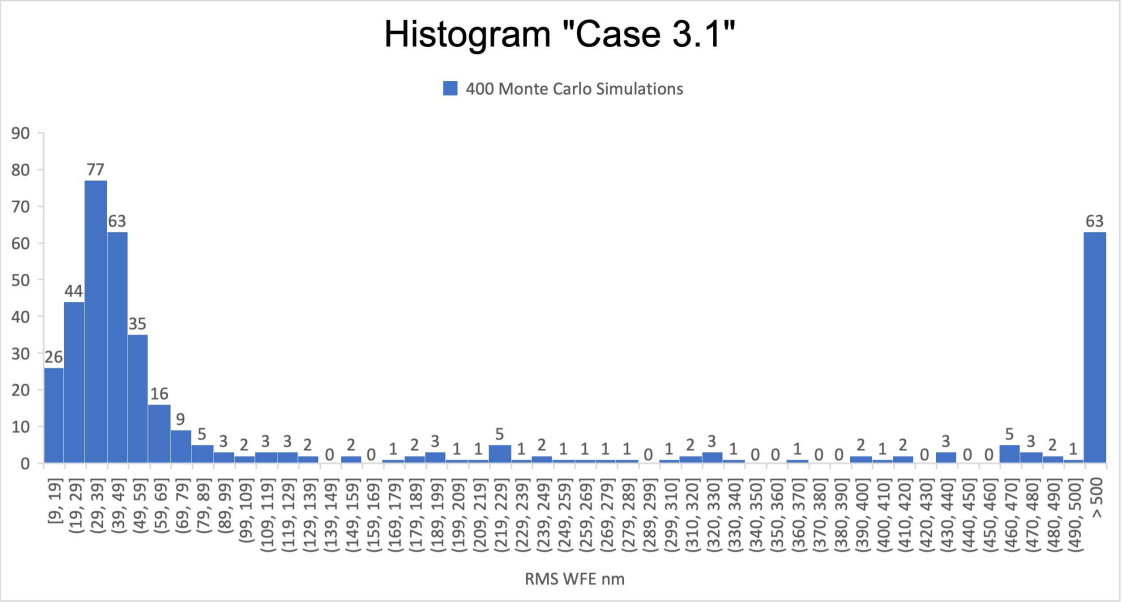

Figure 21: 400 Monte Carlo simulations - “Case 3.1” - Histogram

6.3.1 Worst offenders

Type	Surface	Tolerance	WFE nm	Change nm
TRAD	3	+0.05	1386.75	1372.04
TRAD	3	-0.05	1318.13	1303.4271
TETX	4	-0.05	50.26	35.56
TETX	4	+0.05	50.26	35.56
TETY	4	+0.05	50.26	35.56
TETY	4	-0.05	50.26	35.56
TEDY	4	+0.05	37.22	22.52
TEDY	4	-0.05	37.22	22.52
TEDX	4	+0.05	37.22	22.52
TEDX	4	-0.05	37.22	22.52
TTHI	3-4	+0.1	27.28	12.58
TIRR	3	-0.1	18.09	3.39

Table 16: Worst Offenders "Case 3.1"

6.3.2 Summary of Monte Carlo simulation "Case 3.1"

	RMS WFE (nm)	
Nominal	14.70	
Best	8.74	
Worst	2088.27	
Mean	226.85	
Std Dev		0.0095
COMP_EYE	Thickness [mm]	
Nominal	350.04	
Minimum	348.50	
Maximum	351.50	
Mean	349.96	
Standard Deviation		1.094
COMP_BFD	Thickness [mm]	
Nominal	69.87	
Minimum	68.05	
Maximum	79.97	
Mean	73.46	
Standard Deviation		3.229
RMS WFE Statistics	RMS WFE nm	
90% >	830.51	
80% >	404.30	
50% >	47.12	
20% >	30.11	
10% >	22.67	

Table 17: Summarize of Monte Carlo simulations “Case 3.1” – OpticStudio

6.3.3 Compensator Considerations

As shown in Table (17), the COMP_EYE compensator saturates. Note that COMP_EYE refers to the position of the Eyepiece Assembly and can vary between +/- 1.5 mm (total range of 3 mm) in "Case 3.1". Furthermore in this case:

- COMP_EYE_Nominal = 350.00 mm
- COMP_EYE_Max = 351.50 mm
- COMP_EYE_Min = 348.50 mm

In multiple simulations, the compensator reaches both the maximum and minimum allowable position values. This suggests expanding the position range to determine if it effectively compensates the RMS WFE. Practically, this implies considering a mechanism capable of moving the Eyepiece Assembly over a range greater than 3 mm of displacment.

6.3.4 Case 3.2

It has been observed that "Case 3.1" suggests increasing the compensator's range to mitigate the effect of the tolerance on the primary mirror M1's radius of curvature. Indeed, by expanding this range, the errors are mitigated, and the system approaches the desired performance. This improvement is due to the movement of the Eyepiece Assembly, which, through the COMP_EYE compensator, moves along the telescope's axis until an optimal position is found.
This movement is constrained by the COMP_EYE range. Simulations with various ranges have shown that the shortest range capable of correcting the tolerance is +/- 3 mm (a total range of 6 mm). We will now analyze the results.

- The COMP_EYE is set to ±3.0 mm.

	PARAMETER	**TOLERANCE**
M1	Δ Radius Curvature	±0.05%
M2	Δ Radius Curvature	±0.05%
	Δz	±0.1 mm
	Decenter	±0.05 mm
	Tilt	±0.05°
	Surface Irregularity	±0.1λ
		(λ = 633 nm)
L1,L2,L3	Δ Radius Curvature	±0.1% (precision)
	Δz	±0.1 mm
	Decenter	±0.1 mm
	Tilt	±0.1°
	Surf Irr	±0.1λ PTV
		(λ = 633 nm)
COMPENSATOR	Comp EYE	±3.0 mm
	Comp BFD	68 mm < z < 80 mm

Table 18: Manufacturing and alignment Tolerance of "Case 3.2" configuration

Case 3.2	Nominal	Mean	Median
RMS WFE [nm]	14,70	54,85	36,20

Table 19: 400 Monte Carlo simulations. Nominal, Mean, Median RMS Wave Front Error of "Case 3.2"

Type	Surface	Tolerance	WFE nm	Change nm
TRAD	3	+0.05	228.21	213.51
TRAD	3	-0.05	133.76	119.06
TETX	4	-0.05	50.26	35.56
TETX	4	+0.05	50.26	35.56
TETY	4	+0.05	50.26	35.56
TETY	4	-0.05	50.26	35.56
TEDY	4	+0.05	37.22	22.52
TEDY	4	-0.05	37.22	22.52
TEDX	4	+0.05	37.22	22.52
TEDX	4	-0.05	37.22	22.52
TTHI	3-4	+0.1	27.28	12.58
TIRR	3	-0.1	18.09	3.39

Table 20: Worst Offenders "Case 3.2"

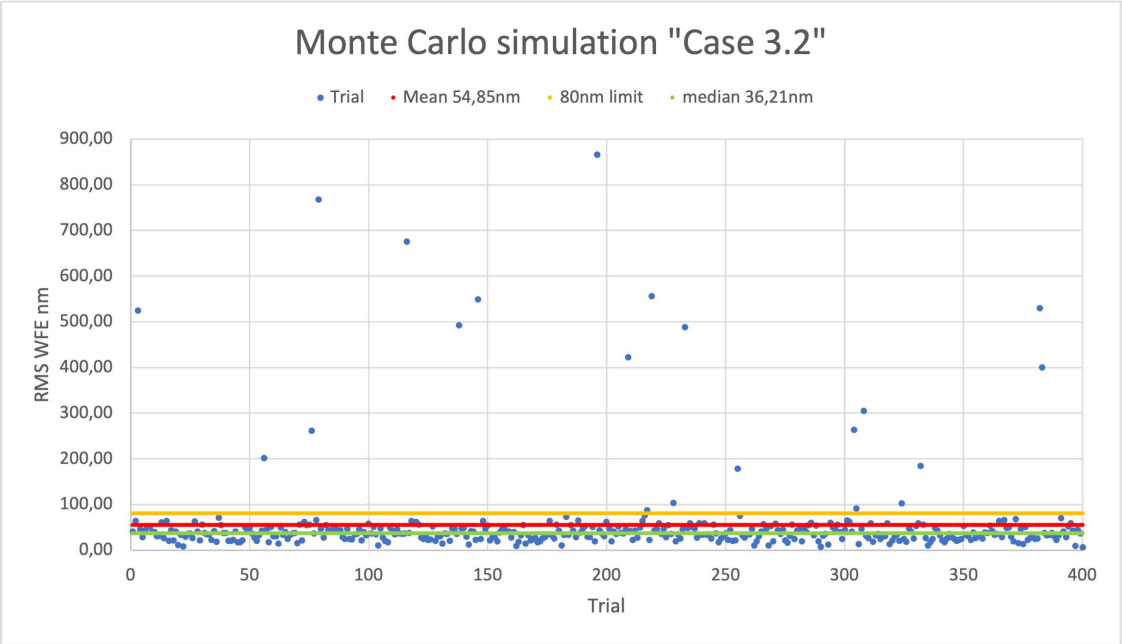

Figure 22: 400 Monte Carlo simulations - “Case 3.2” - Scatter Diagram

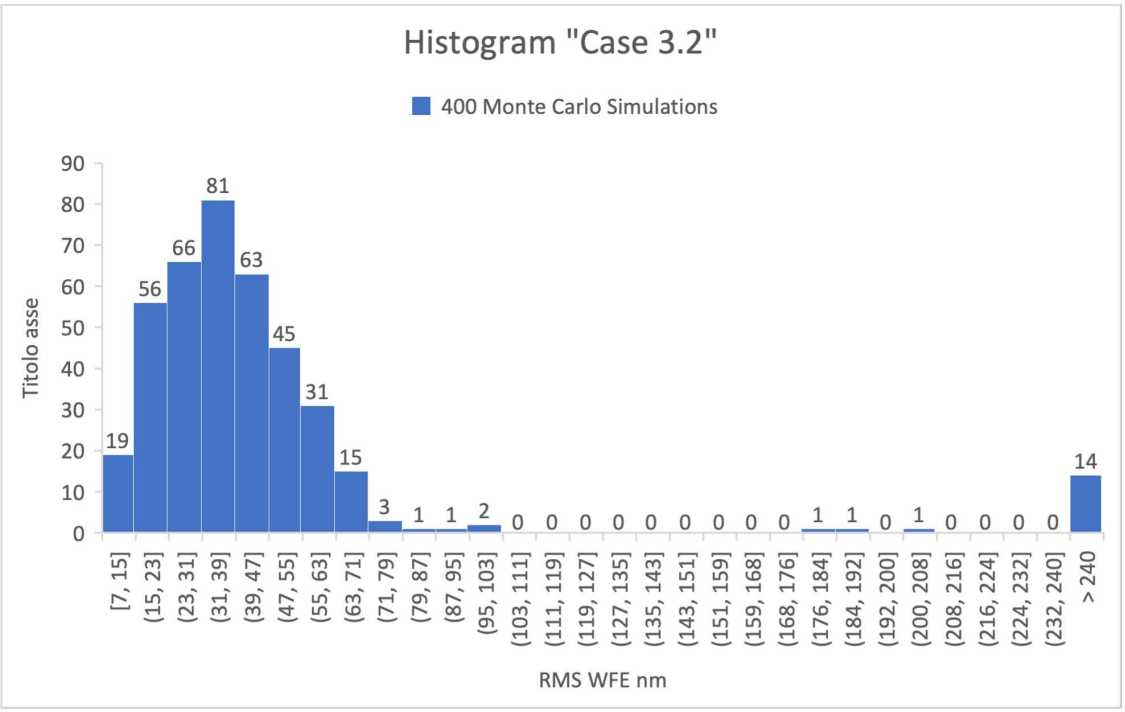

Figure 23: 400 Monte Carlo simulations - “Case 3.2” - Histogram

6.3.5 Results Review

Compared to the previous "Case 3.1," we obtained a better distribution of results. 94.5% of the results meet the requirement of 80 nm WFE. However, there are 12 simulations where the wavefront error exceeds 300 nm, with peaks reaching 850 nm. This indicates that the COMP_EYE compensator successfully corrected most of the errors present in previous "Case 3.1" It is important to note that in this "Case 3.2," a compensator with a 6 mm range was considered. Therefore, the feasibility of its implementation needs to be evaluated.

6.4 Case 4

Let's now consider adding a Solar Filter (SF) to our optical system. We will analyze how the telescope's performance changes and conduct a study on the tolerances of the telescope system with the solar filter. To control the telescope's thermal conditions under sunlight exposure and to protect its internal optical components from the radiative environment of space and possible contamination from the ground, a Solar Filter (SF) is installed at the telescope's entrance.
The characteristics of the Solar Filter are derived from the telescope's requirements, and only the most relevant ones for the analysis are listed here.

- **Flat surface:** The SF should consist of a flat window.
- **Dimensions:** The optical clear aperture of the SF shall match the telescope's aperture of 250 mm +1.00 / -0.00 in diameter.
- **Tilt:** The SF shall be mounted with its normal axis tilted 0.5 degrees with respect to the telescope optical axis to prevent back reflections of the transmitted laser beam.
- **Material:** The substrate material shall be Corning C79-80 high purity fused silica, or equivalent.
- **Thickness:** There is no specific requirement on the thickness of the SF. However, a range of 7-8 mm may be considered.
- **Band Pass Coating:** The outer surface shall be protected by a Band Pass Coating.
- **Anti-Reflective Coating:** The inner surface shall be covered by an Anti-Reflective Coating (AR).

After studying the requirements and making some considerations, a glass from the SUPRASIL® family was chosen as the SF's material. It is a synthetic pure silica glass with high performance in the infrared. The SF thickness is set to 7 mm. In this analysis, the internal and external coatings are not considered.

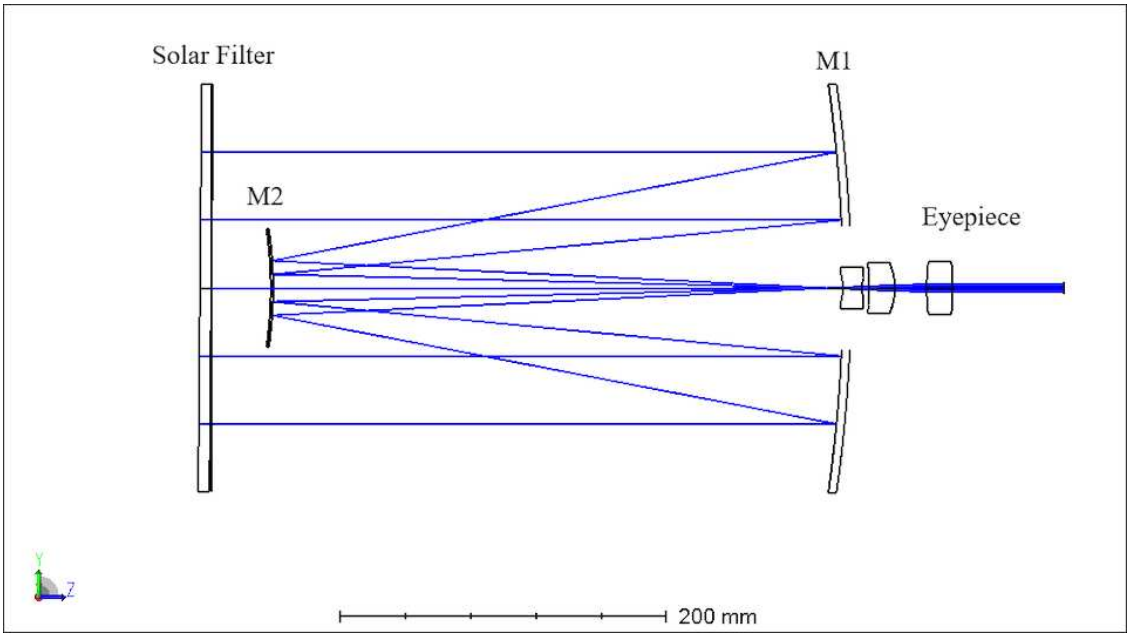

Figure 24: Optical Design with Solar Filter - OpticStudio

6.4.1 Tolerances

Let's now conduct a tolerance analysis ("Case 4") of the overall system consisting the Solar Filter (SF), the mirrors (M1, M2), and the Eyepiece Assembly (L1, L2, L3). This analysis considers the tolerances of "Case 1" (refer to Table (4)) along with the manufacturing and alignment tolerances of the SF shown in Table (21).

	PARAMETER	**TOLERANCE**
SF	Flatness	$\pm 1\lambda$
	Δz	± 0.1 mm
	Decenter	± 0.1 mm
	Tilt	$\pm 0.1°$
	Surface Irregularity	$\pm 0.1\lambda$ PTV
		($\lambda = 633$ nm)

Table 21: Manufacturing and alignment Tolerance of Solar Filter

Surface "Flatness" measures the deviation of a flat surface using an optical flat, a high-

precision reference surface. The flatness is determined by examining the fringes formed when the test surface is placed against the optical flat. Deviations are measured in waves (λ = 633 nm), with 1λ flatness being typical grade, $\lambda/4$ as precision grade, and $\lambda/20$ as high precision grade. The Solar Filter has a flatness tolerance of 1λ.
The introduction of the filter, a flat parallel-faced plate tilted at 0.5°, should not significantly impact the telescope's performance in terms of RMS WFE. Preliminary analyses using the WaveFront Map and Spot Diagram (utilizing a paraxial focus as in section (4)) confirm this hypothesis. Furthermore, analogous result to "Case 1" is expected in the tolerance analysis, as the manufacturing and alignment parameters of the filter are not expected to significantly affect the system.

6.4.2 Monte Carlo simulation

Below, we present the results of the Monte Carlo analysis for "Case 4" compared with "Case 1".

Case 4	Nominal	Mean	Median
RMS WFE [nm]	14,70	38,17	33,64

Case 1	Nominal	Mean	Median
RMS WFE [nm]	14,70	40,62	35,75

Table 22: 400 Monte Carlo simulations. Nominal, Mean, Median RMS Wave Front Error of "Case 4" and "Case 1"

As can be observed from the scatter diagrams (Figure (25)) and histograms (Figure (27)), the addition of the Solar Filter does not result in any changes to the telescope's RMS WFE. We can therefore conclude that the Solar Filter does not introduce any critical tolerances to the system, does not present any particular issues, and can be integrated into the optical system without concerns.

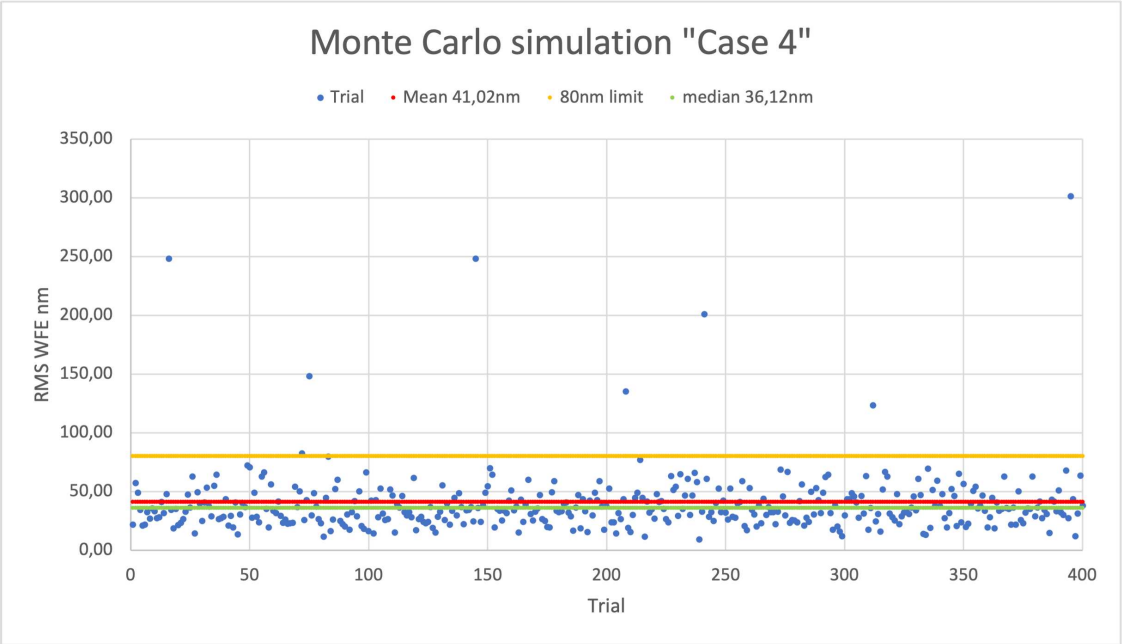

Figure 25: 400 Monte Carlo simulations - “Case 4” - Scatter Diagram

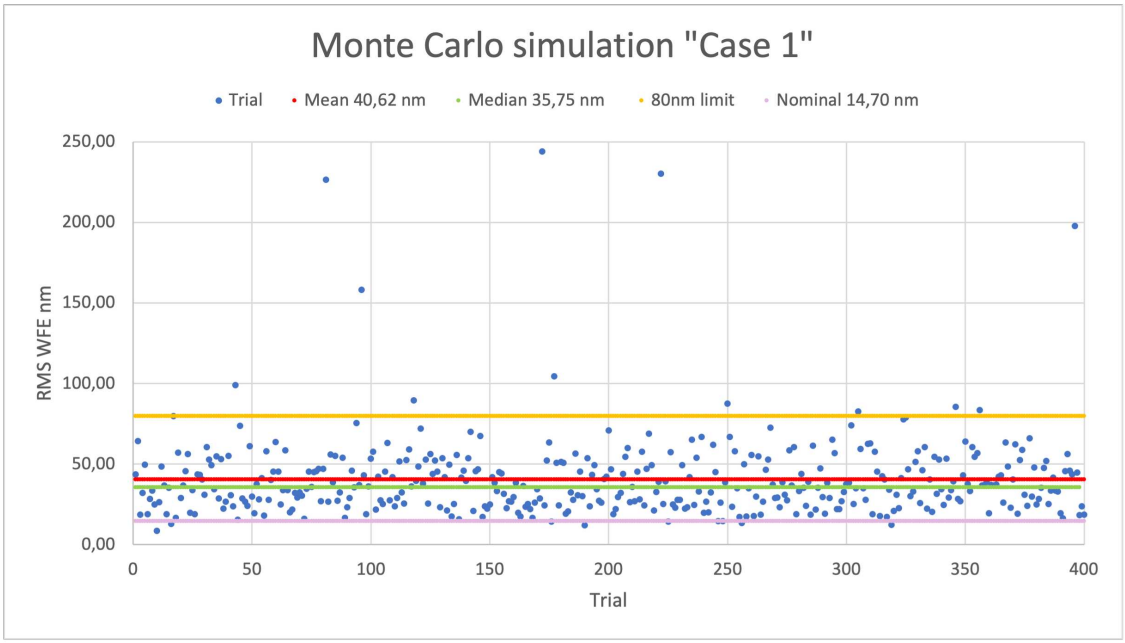

Figure 26: 400 Monte Carlo simulations - “Case 1” - Scatter Diagram

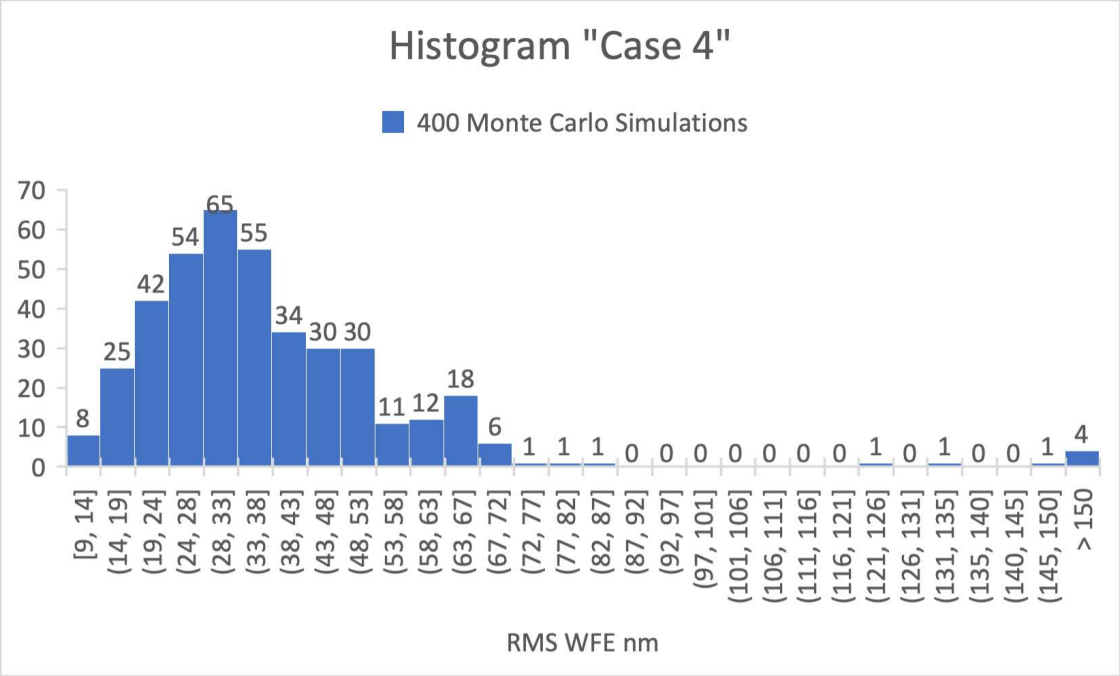

Figure 27: 400 Monte Carlo simulations - “Case 4” - Histogram

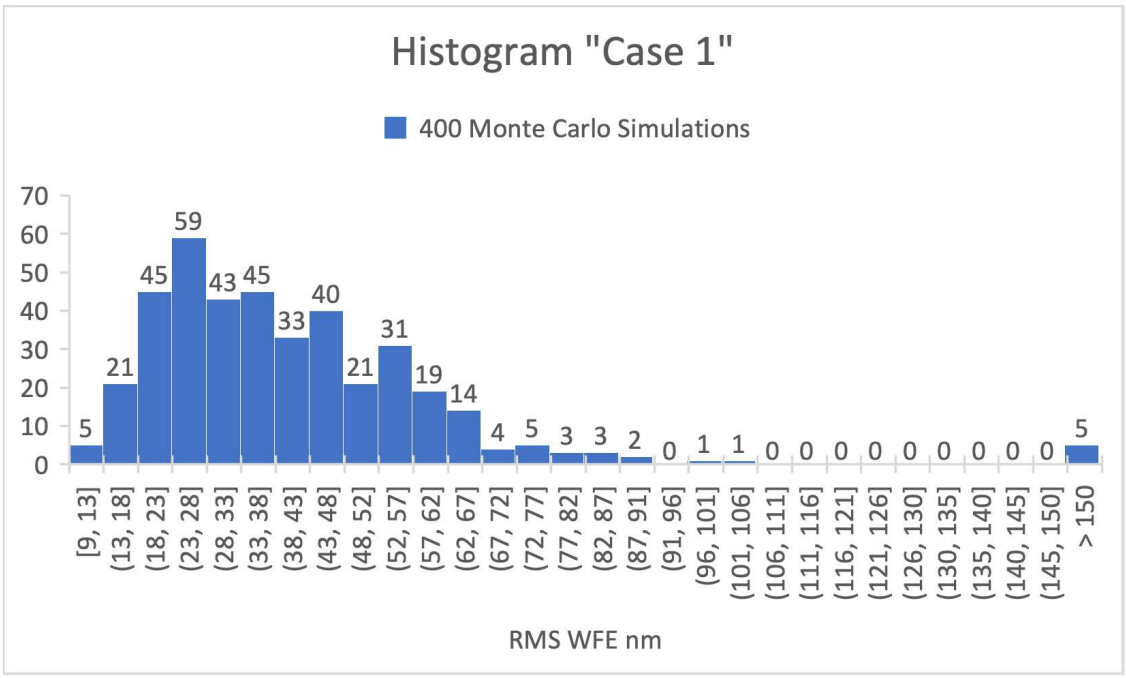

Figure 28: 400 Monte Carlo simulations - “Case 1” - Histogram

7 Conclusions

The aim of this thesis is to define the manufacturing and alignment tolerances for the Spock Ø250mm telescope, an essential step in the instrument's design. Through detailed tolerance analysis, critical parameters affecting the telescope's performance, such as the radius of curvature of the M1 and M2 mirrors and the tilt and decenter of M2, have been identified. The results from simulations and sensitivity analysis have shown how variations in these parameters can significantly impact the optical performance of the system.

Furthermore, this study demonstrates how the axial positioning of the entire Eyepiece Assembly can be effectively used as a compensator (COMP_EYE) to mitigate tolerances, particularly the radius of curvature of the mirrors.

Since the position of the exit pupil is not yet known, the simulations were performed using a wide range for the COMP_BFD parameter. As explained in the compensators paragraph (5.2), since the optical system is afocal, the range of this compensator and, consequently, the position of the exit pupil do not significantly impact the telescope's performance, so all obtained results can be considered valid. When the telescope is integrated and this information becomes available, the range will be refined.

The tolerances defined in this thesis guide the manufacturing process by providing indications on the geometric characteristics, materials, and surface irregularities of optical surfaces. "Case 4", which is essentially "Case 1" with the addition of the solar filter, proves to be an excellent trade-off between instrument performance and manufacturing costs. Monte Carlo analyses have validated the tolerances, demonstrating that the instrument meets the requirements.

Below there is the summary tolerance, Table (23), for "Case 4". Furthermore, the optical surfaces used in OpticStudio ("Lens Data") are represented in Table (24) and in the figure(29). "Tolerance Data Editor", in Table(25), describes the tolerances of each individual optical surface analyzed in the software.

	PARAMETER	**TOLERANCE**
M1,M2	Δ Radius Curvature	$\pm 0.01\%$
	Δz	$\pm 0.1\,\mathrm{mm}$
	Decenter	$\pm 0.05\,\mathrm{mm}$
	Tilt	$\pm 0.05^\circ$
	Surface Irregularity	$\pm 0.1\lambda$
		$(\lambda = 633\,\mathrm{nm})$
L1,L2,L3	Δ Radius Curvature	$\pm 0.1\%$
	Δz	$\pm 0.1\,\mathrm{mm}$
	Decenter	$\pm 0.1\,\mathrm{mm}$
	Tilt	$\pm 0.1^\circ$
	Surf Irr	$\pm 0.1\lambda$ RMS
		$(\lambda = 633\,\mathrm{nm})$
SF	Flatness	$\pm 1\lambda$
	Δz	$\pm 0.1\,\mathrm{mm}$
	Decenter	$\pm 0.1\,\mathrm{mm}$
	Tilt	$\pm 0.1^\circ$
	Surface Irregularity	$\pm 0.1\lambda$ PTV
		$(\lambda = 633\,\mathrm{nm})$
COMPENSATOR	Comp EYE	$\pm 1.5\,\mathrm{mm}$
	Comp BFD	$68\,\mathrm{mm} < z < 80\,\mathrm{mm}$

Table 23: Manufacturing and alignment Tolerance of "Case 4"

SURF	Type	Comment	Radius	Thickness	Material	Semi-Diameter	Tilt (°)
0	STD	Object	∞	100.00		0.00	
1	STD		∞	50.00		125.00	
2	CBRK	Tilt	∞	0.00		0.00	0.50
3	STD	FRONT SF	∞	7.00	SUPRASIL	125.00	
4	STD	REAR SF	∞	-7.00		125.05	
5	CBRK	Tilt	∞	7.00		0.00	0.50
6	STD	Dummy	∞	388.00		125.02	
7	STD	M1	-875.00	-350.00	MIRROR	125.24	
8	STD	M2	-236.00	350.00	MIRROR	36.32	
9	STD	FRONT L1	-29.00	12.06	SK-1300	8.77	
10	STD	REAR L1	164.00	3.74		12.51	
11	STD	FRONT L2	-335.00	16.13	S-LAL20	13.26	
12	STD	REAR L2	-38.40	19.56		15.31	
13	STD	FRONT L3	133.00	16.04	S-LAH58	15.95	
14	STD	REAR L3	-142.00	68.01		15.95	
15	STD	EP	∞	0.00		3.75	

Table 24: Optical surfaces specifications - "Lens Data" - OpticStudio.

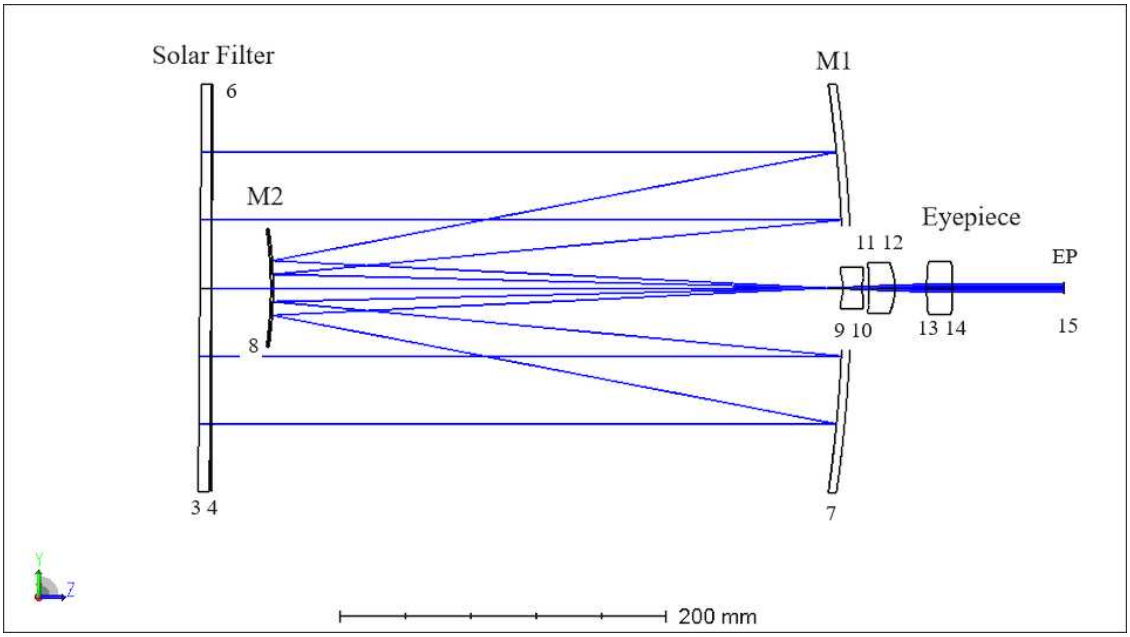

Figure 29: Optical Design Layout and Solar Filter - OpticStudio.

Table 25: Tolerance Data "Case 4" - all Manufacturing and Alignment Tolerances data of every element/surface - Zemax OpticStudio

Type	Int1	Int2	Nominal	Min	Max	Comment
COMP	8	0	350	-1.5	1.5	COMP_EYE
COMP	14	0	68.007	0	12	COMP_BFD
TWAV			0.633			Default test wavelength.
TRAD	3	0	Infinity	-0.1	0.1	Default radius tolerances.
TRAD	4	0	Infinity	-0.1	0.1	
TRAD	7	1	-875.001	-1.00E-02	1.00E-02	
TRAD	8	1	-235.637	-1.00E-02	1.00E-02	
TRAD	9	1	-28.981	-0.1	0.1	
TRAD	10	1	164.385	-0.1	0.1	
TRAD	11	1	-334.512	-0.1	0.1	
TRAD	12	1	-38.401	-0.1	0.1	
TRAD	13	1	132.653	-0.1	0.1	
TRAD	14	1	-141.612	-0.1	0.1	
TTHI	3	4	7	-0.1	0.1	Default thickness tolerances.
TTHI	4	5	-7	-0.1	0.1	
TTHI	6	6	388	-0.1	0.1	
TTHI	7	8	-350	-0.1	0.1	
TTHI	8	10	350	-0.1	0.1	
TTHI	9	10	12.056	-0.1	0.1	
TTHI	10	12	3.74	-0.1	0.1	
TTHI	11	12	16.125	-0.1	0.1	
TTHI	12	14	19.555	-0.1	0.1	
TTHI	13	14	16.036	-0.1	0.1	
TEDX	3	4	0	-0.1	0.1	Default element dec/tilt tolerances 3-4.
TEDY	3	4	0	-0.1	0.1	
TETX	3	4	0	-0.1	0.1	
TETY	3	4	0	-0.1	0.1	
TEDX	8	8	0	-0.05	0.05	Default element dec/tilt tolerances 8-8.
TEDY	8	8	0	-0.05	0.05	
TETX	8	8	0	-0.05	0.05	
TETY	8	8	0	-0.05	0.05	

Type	Int1	Int2	Nominal	Min	Max	Comment
TEDX	9	10	0	-0.1	0.1	Default element dec/tilt tolerances 9-10.
TEDY	9	10	0	-0.1	0.1	
TETX	9	10	0	-0.1	0.1	
TETY	9	10	0	-0.1	0.1	
TEDX	11	12	0	-0.1	0.1	Default element dec/tilt tolerances 11-12.
TEDY	11	12	0	-0.1	0.1	
TETX	11	12	0	-0.1	0.1	
TETY	11	12	0	-0.1	0.1	
TEDX	13	14	0	-0.1	0.1	Default element dec/tilt tolerances 13-14.
TEDY	13	14	0	-0.1	0.1	
TETX	13	14	0	-0.1	0.1	
TETY	13	14	0	-0.1	0.1	
TSDX	3		0	-0.1	0.1	Default surface dec/tilt tolerances 3.
TSDY	3		0	-0.1	0.1	
TSTX	3		0	-0.017	0.017	
TSTY	3		0	-0.017	0.017	
TSDX	4		0	-0.1	0.1	Default surface dec/tilt tolerances 4.
TSDY	4		0	-0.1	0.1	
TSTX	4		0	-0.017	0.017	
TSTY	4		0	-0.017	0.017	
TSDX	9		0	-0.1	0.1	Default surface dec/tilt tolerances 9.
TSDY	9		0	-0.1	0.1	
TSTX	9		0	-0.017	0.017	
TSTY	9		0	-0.017	0.017	
TSDX	10		0	-0.1	0.1	Default surface dec/tilt tolerances 10.
TSDY	10		0	-0.1	0.1	
TSTX	10		0	-0.017	0.017	
TSTY	10		0	-0.017	0.017	
TSDX	11		0	-0.1	0.1	Default surface dec/tilt tolerances 11.
TSDY	11		0	-0.1	0.1	

Type	Int1	Int2	Nominal	Min	Max	Comment
TSTX	11		0	-0.017	0.017	
TSTY	11		0	-0.017	0.017	
TSDX	12		0	-0.1	0.1	Default surface dec/tilt tolerances 12.
TSDY	12		0	-0.1	0.1	
TSTX	12		0	-0.017	0.017	
TSTY	12		0	-0.017	0.017	
TSDX	13		0	-0.1	0.1	Default surface dec/tilt tolerances 13.
TSDY	13		0	-0.1	0.1	
TSTX	13		0	-0.017	0.017	
TSTY	13		0	-0.017	0.017	
TSDX	14		0	-0.1	0.1	Default surface dec/tilt tolerances 14.
TSDY	14		0	-0.1	0.1	
TSTX	14		0	-0.017	0.017	
TSTY	14		0	-0.017	0.017	
TIRR	3		0	-0.1	0.1	Default irregularity tolerances.
TIRR	4		0	-0.1	0.1	
TIRR	7		0	-0.1	0.1	
TIRR	8		0	-0.1	0.1	
TIRR	9		0	-0.1	0.1	
TIRR	10		0	-0.1	0.1	
TIRR	11		0	-0.1	0.1	
TIRR	12		0	-0.1	0.1	
TIRR	13		0	-0.1	0.1	
TIRR	14		0	-0.1	0.1	
TIND	3		1.458	-5.00E-04	5.00E-04	Default index tolerances.
TIND	9		1.459	-5.00E-04	5.00E-04	
TIND	11		1.699	-5.00E-04	5.00E-04	
TIND	13		1.883	-5.00E-04	5.00E-04	
TABB	3		67.878	-0.193	0.193	Default Abbe tolerances.
TABB	9		67.837	-0.204	0.204	
TABB	11		51.112	-0.153	0.153	
TABB	13		40.765	-0.122	0.122	

8 Bibliography - Sitography

1. Ansys Zemax OpticStudio 2023 R2 - User Manual.
2. A. Bacco, G. Naletto, G. Rodeghiero, C. Gargano - ASTRI Stellar Intensity Interferometry Instrument: analisi delle tolleranze optomeccaniche.
3. Da Deppo, Vania; Middleton, Kevin; Focardi, Mauro; Morgante, Gianluca; Grella, Samuele; - The afocal telescope optical design and tolerance analysis for the ESA ARIEL mission.
4. E. Hecht, Optics, Pearson Addison Wesley
5. M.C.E. Huber, A. Pauluhn, J.L. Culhane, J.G. Timothy, K. Wilhelm, A. Zehnder (Eds.), Observing Photons in Space – A guide to Experimental Space Astronomy, International Space Science Institute, 2013.
6. https://support.zemax.com/hc/en-us/articles/1500005576982-How-to-perform-a-sequential-tolerance-analysis/
7. https://www.edmundoptics.com/knowledge-center/application-notes/optics/understanding-optical-specifications/
8. https://newsroom.enginsoft.com/tolleranze-dimensionali-e-tolleranze-geometriche
9. https://www.heraeus-conamic.com/brands/suprasil
10. https://www.ohara-gmbh.com/fileadmin/user_upload/pdfs/SK-1300.pdf
11. https://oharacorp.com/glass-type/s-lal/
12. https://oharacorp.com/glass/s-lah58/